AD-A074 838 PHYSICS INTERNATIONAL CO SAN LEANDRO CA F/G 20/14
PULSER FOR VERTICALLY POLARIZED DIPOLE FACILITY (VPD-II).(U)
JUL 79 F29601-76-C-0048
UNCLASSIFIED PIFR-900 AFWL-TR-78-243 NL

1 OF 1
AD A074838

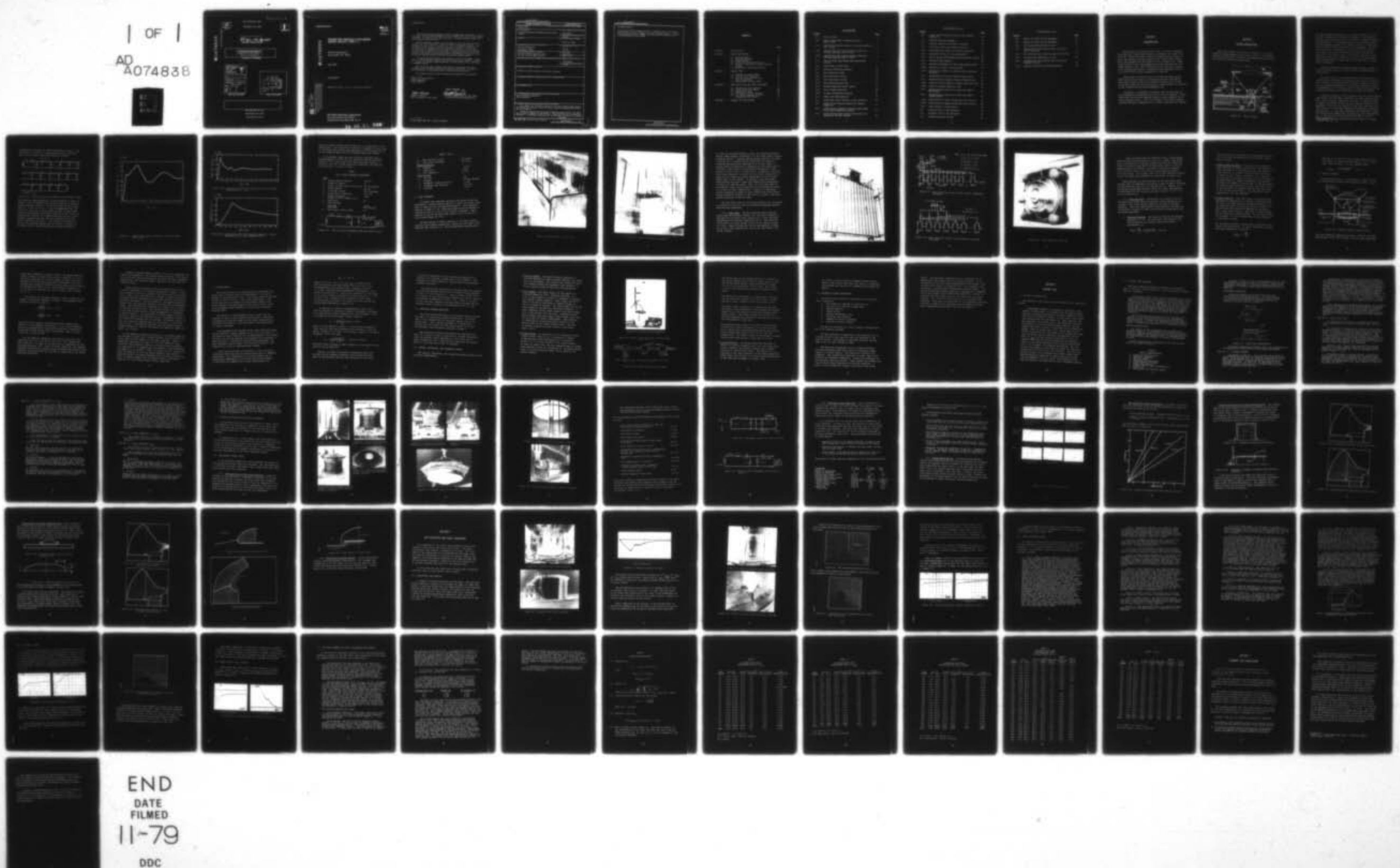

END
DATE FILMED
11-79
DDC

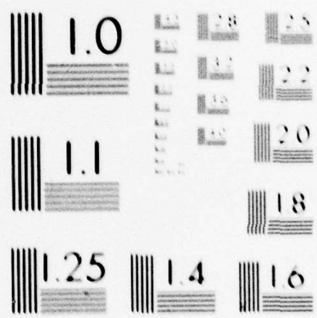

MICROCOPY RESOLUTION TEST CHART
NATIONAL BUREAU OF STANDARDS-1963-A

AD-E200365

DATA PROCESSING SHEET

PHOTOGRAPH THIS SHEET

III

LEVEL

I

INVENTORY

AD A074838

DDC ACCESSION NUMBER

AFWL-TR-78-243

DOCUMENT IDENTIFICATION

DISTRIBUTION STATEMENT A

Approved for public release;
Distribution Unlimited

DISTRIBUTION STATEMENT

Accession For	
NTIS GRA&I	X
DDC TAB	
Unannounced	
Justification	
By	
Distribution/	
Availability Codes	
Dist.	Avail and/or special
A	

DISTRIBUTION STAMP

DDC

RECEIVED

OCT 9 1979

D

DATE ACCESSIONED

DATE RECEIVED IN DDC

PHOTOGRAPH THIS SHEET

AND RETURN TO DDA-2

AFWL-TR-78-243

PULSER FOR VERTICALLY POLARIZED DIPOLE FACILITY (VPD-11)

Physics International
San Leandro, CA 94577

July 1979

Final Report

Approved for public release; distribution unlimited.

AIR FORCE WEAPONS LABORATORY
Air Force Systems Command
Kirtland Air Force Base, NM 87117

This final report was prepared by Physics International, San Leandro, California, under Contract F29601-76-C-0048, Job Order 12090401 with the Air Force Weapons Laboratory, Kirtland Air Force Base, New Mexico. Mr Edsal Chappelle (ELSD) was the Laboratory Project Officer.

This technical report has been reviewed and is approved for publication.

Edsal Chappelle
EDSAL CHAPPELLE
Project Officer

FOR THE COMMANDER

Albert B. Griffin
ALBERT B. GRIFFIN
Chief, Simulation & Test Branch

Harold O. Spurlin
HAROLD O. SPURLIN, Lt Col, USAF
Acting Chief, Electromagnetics Div

UNCLASSIFIED

SECURITY CLASSIFICATION OF THIS PAGE (When Data Entered)

REPORT DOCUMENTATION PAGE

READ INSTRUCTIONS BEFORE COMPLETING FORM

1. REPORT NUMBER: AFWL-TR-78-243	2. GOVT ACCESSION NO. / 3. RECIPIENT'S CATALOG NUMBER
4. TITLE (and Subtitle): PULSER FOR VERTICALLY POLARIZED DIPOLE FACILITY (VPD-II)	5. TYPE OF REPORT & PERIOD COVERED: Final Report
	6. PERFORMING ORG. REPORT NUMBER: PIFR-900
7. AUTHOR(s)	8. CONTRACT OR GRANT NUMBER(s): F29601-76-C-0048
9. PERFORMING ORGANIZATION NAME AND ADDRESS: Physics International, 2700 Merced Street, San Leandro CA 94577	10. PROGRAM ELEMENT, PROJECT, TASK AREA & WORK UNIT NUMBERS: 64747F, 12090401
11. CONTROLLING OFFICE NAME AND ADDRESS: Air Force Weapons Laboratory (ELS), Kirtland Air Force Base, NM 87117	12. REPORT DATE: July 1979
	13. NUMBER OF PAGES: 74
14. MONITORING AGENCY NAME & ADDRESS (if different from Controlling Office)	15. SECURITY CLASS. (of this report): UNCLASSIFIED
	15a. DECLASSIFICATION/DOWNGRADING SCHEDULE

16. DISTRIBUTION STATEMENT (of this Report)

Approved for public release; distribution unlimited.

17. DISTRIBUTION STATEMENT (of the abstract entered in Block 20, if different from Report)

18. SUPPLEMENTARY NOTES

19. KEY WORDS (Continue on reverse side if necessary and identify by block number)

High Voltage Marx Generators
Pulse Generators

20. ABSTRACT (Continue on reverse side if necessary and identify by block number)

This report will provide an outline of the pulser system design features and will give an account of both the factory and site acceptance test procedures and results.

During the testing periods certain modifications were found to be necessary in order to improve the performance. These modifications are described. Ultimately, a performance limitation was realized when the pulser was operated

Continued

Continued Item 20.

into the full VPD-II antenna structure, a limitation which could not be removed without a major redesign of the output peaking circuit. This will be discussed in the report summary and some tentative suggestions for a future up-grading will be offered.

CONTENTS

ILLUSTRATIONS

ILLUSTRATIONS (cont.)

ILLUSTRATIONS (cont.)

SECTION 1

INTRODUCTION

The Vertically Polarized Dipole (VPD) II pulser procurement was awarded to Physics International in December 1975 under Contract No. F29601-76-C-0048. After an extensive factory test, in which the pulser system was operated into a dummy load arrangement, the equipment was delivered to site in August 1977. After installation on site, the equipment was again operated into the dummy resistive load, now integrated into the main conic section of the antenna gas housing. Acceptance test procedures started on 18 April 1978 and were completed on 5 May 1978.

During both the factory and site testing periods, certain modifications were found to be necessary and were implemented. This report gives an account of these modifications as it describes the system and the chronological events between the awarding of the contract and the final acceptance test.

Ultimately, a performance limitation was realized when the pulse generator was operated into the full VPD II antenna, a limitation which could not be removed without a major redesign of the output peaking circuit. This is discussed in the report summary and some tentative suggestions for a future up-grading are offered.

SECTION 2

SYSTEM DESCRIPTION

The pulser system, illustrated in Figure 2-1, is a Marx generator peaking-capacitor electrical circuit. The peaking capacitor is physically located in and approximately co-planar with the VPD II facility ground plane.

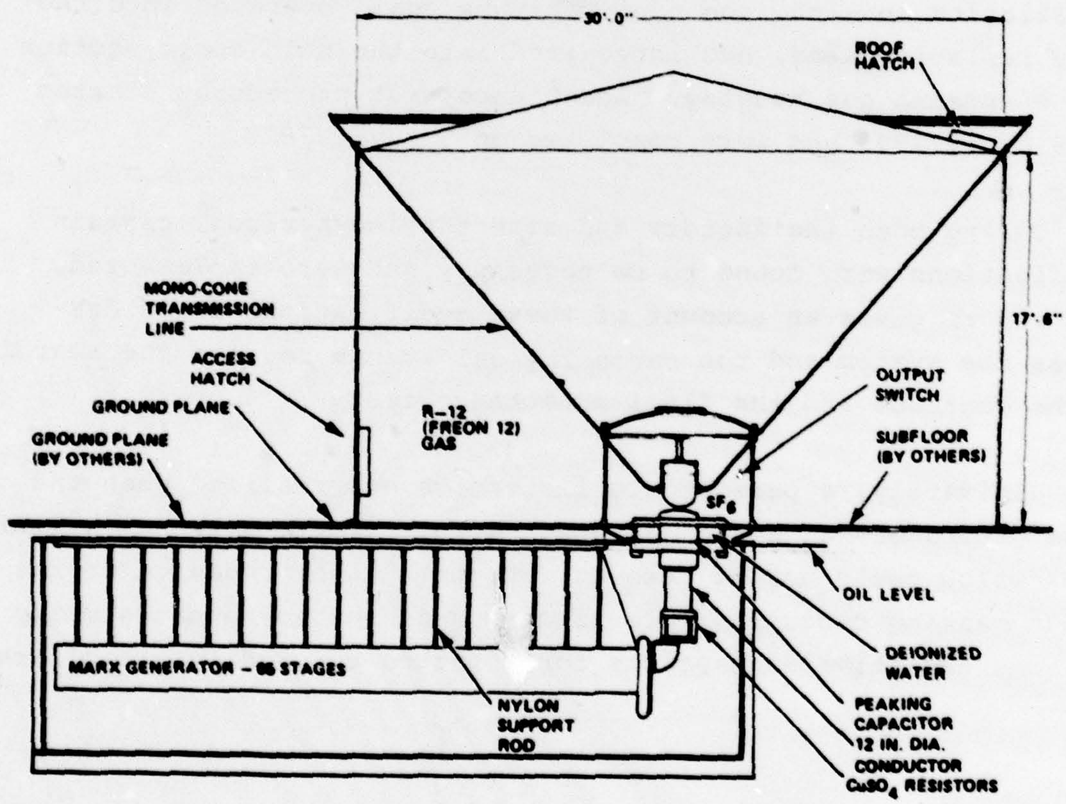

Figure 2-1 VPD II Pulser.

The peaking-capacitor design is a low wave impedance, low inductance, compact water dielectric capacitor. Its design is similar, but scaled up in size, to the RES I transfer capacitor. The compactness of the peaking-capacitor is made possible by the half-symmetry nature of the VPD-II facility in conjunction with the known polarity effect for water breakdown. The preferred polarity of operation (i.e., the mono-cone negative with respect to ground) preferentially places the peaking-capacitor in the ground plane, which offers additional advantages, principally with regard to structural considerations since the mono-cone, in this case, is not required to contain pulser components.

The water dielectric peaking-capacitor feeds a uniform 60-ohm mono-cone by way of a self-closing, pressurized-SF_6 gas output switch.

The mono-cone is a continuous conducting structure contained within a dielectric enclosure filled with R-12 (Freon 12) gas to electrically insulate the conducting surfaces until the electric fields associated with the highest operating voltage have decreased to a low enough value to permit safe exit of the conducting surfaces into the ambient air dielectric medium.

A peaking-capacitor circuit supplies the fast-rising initial load current that the Marx, because of its stray series inductance, cannot directly supply into the load. A peaking circuit is ideally applicable to circuits with constant resistive load impedances. The fact that the VPD II facility mono-cone is an "open circuit" in late time suggests the presence of late-time oscillations; i.e., the Marx inductance can potentially "ring" with the parallel combination of peaking (C_p) and load capacity (C_l).* For the ideal voltage-source-fed peaking circuit,

*This assumes that the Marx-erected series capacity is large compared with $C_p + C_l$.

illustrated in Figure 2-2, such oscillations do exist. The mono-cone in this case is represented by 15 L-C sections, each 12 ns (12 feet) long with resistive grading.

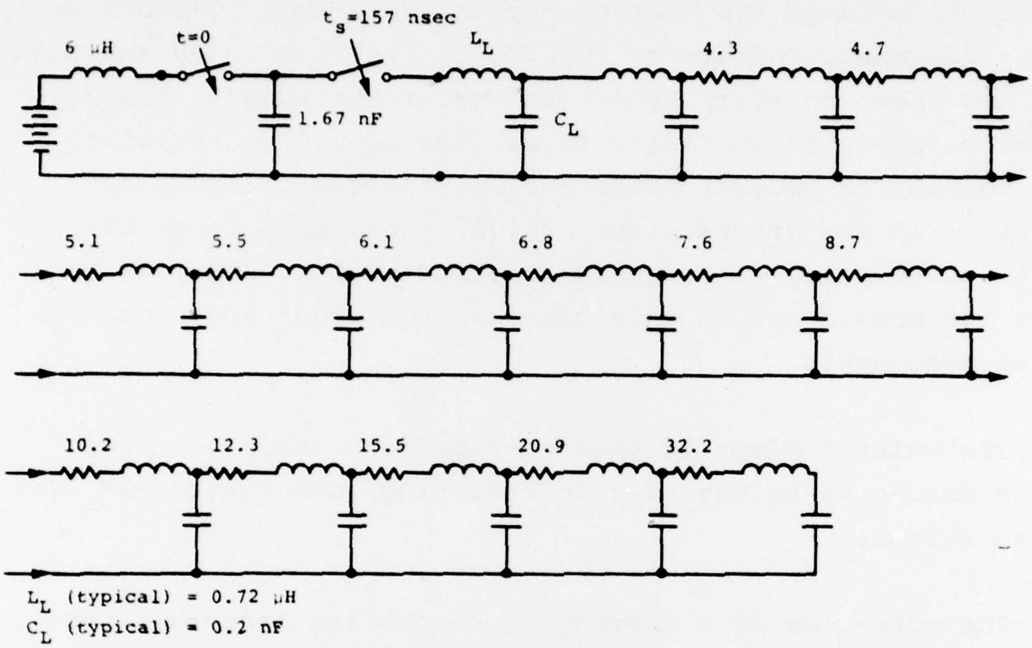

Figure 2-2 Step voltage source peaking circuit--VPD II load.

The resulting peaking-capacitor voltage waveform is shown in Figure 2-3 for an assumed 6-μH series inductance in which the peaking capacitor value is 1.67 nF and output switch closure time ($t_s = \pi/2\omega$) is 157 ns. It must be emphasized that the circuit in this case is driven from an ideal voltage source and that the late-time oscillatory behavior of the circuit is substantially reduced for a capacitively fed circuit (illustrated in Figures 2-4a and 2-4b for a modified electrical circuit shown in Figure 2-5). The circuits of Figures 2-2 and 2-5 are identical except that the circuit in Figure 2-5 is driven from a 3.50-nF source and the peaking capacitor

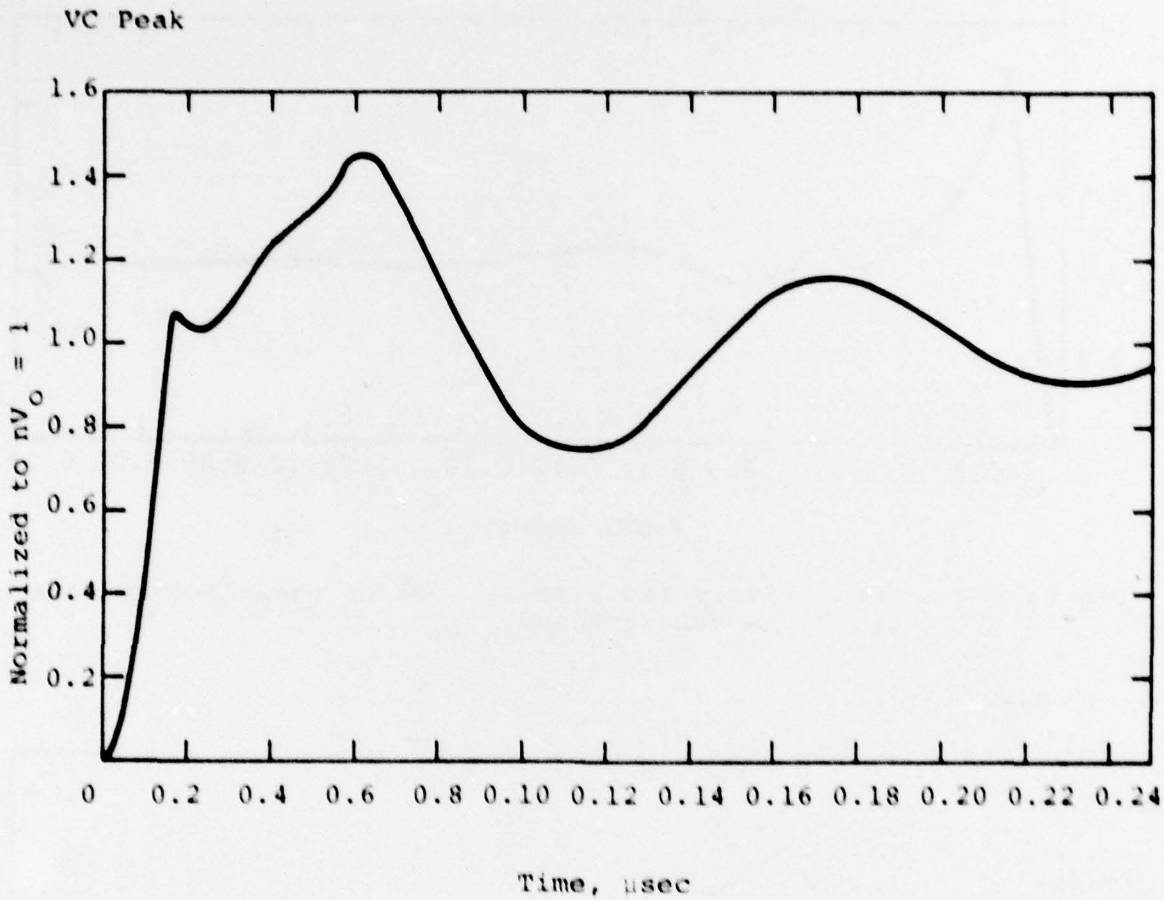

Figure 2-3 Step source peaking capacitor voltage waveform--VPD II load.

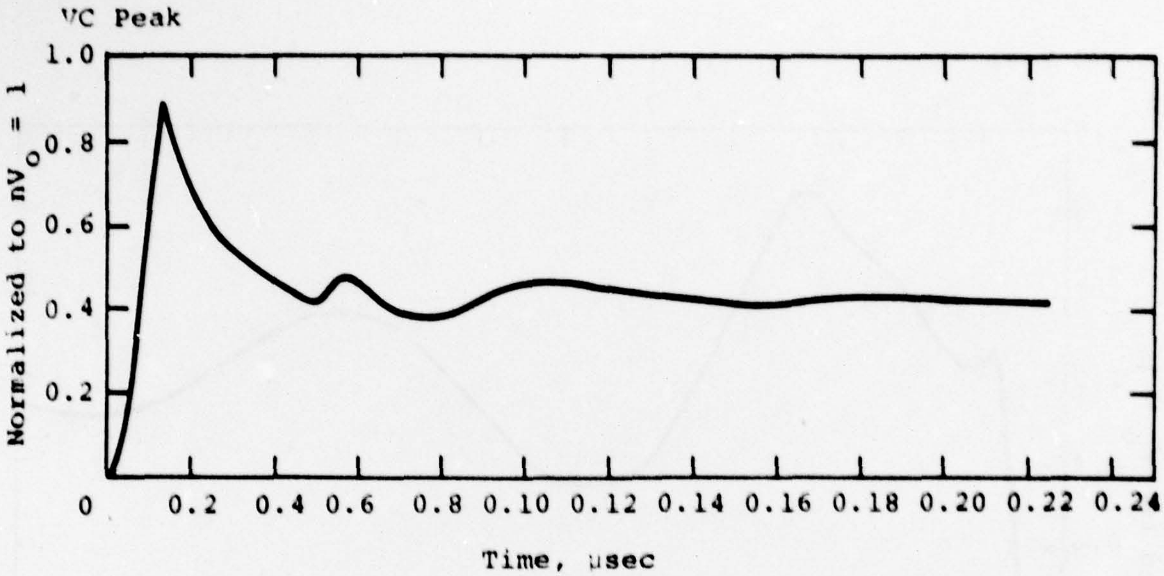

Figure 2-4a Capacitively fed circuit-peaking capacitor voltage waveform--VPD II load.

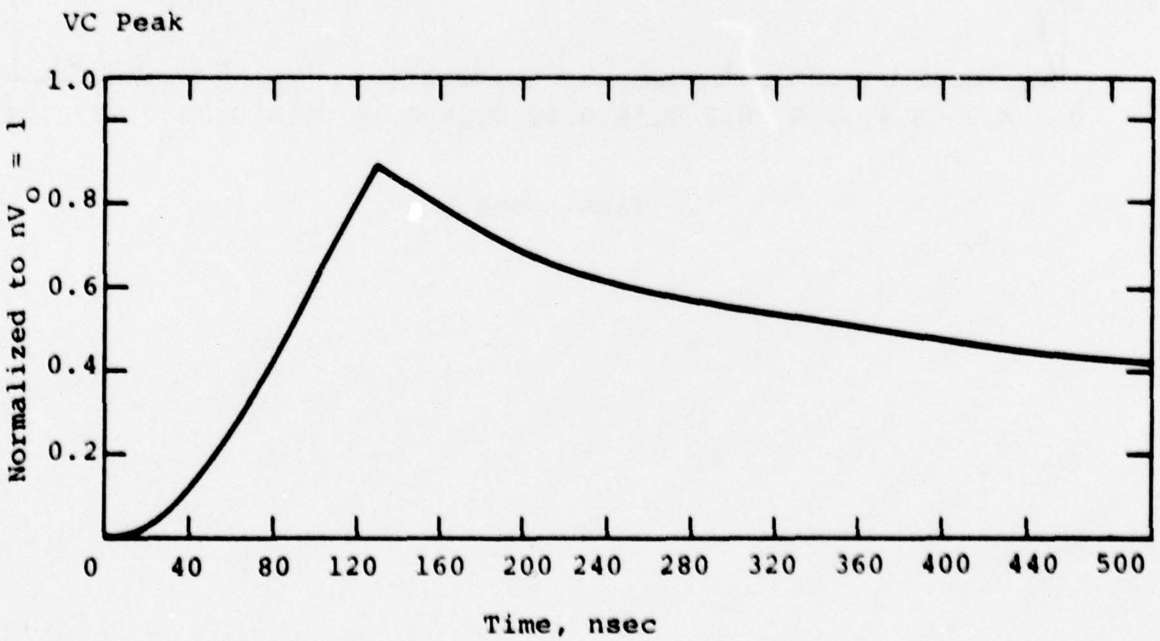

Figure 2-4b Capacitively fed circuit-peaking capacitor voltage waveform--VPD II load (expanded scale).

value and output switch closure time are 1.1 nF and about 130 ns, respectively. The waveform in Figure 4b is expanded in early time to illustrate more clearly peaking-capacitor pulse charge and the initial waveform decay into the simulator mono-cone antenna.

We concluded, based upon the preceding analyses, that a peaking-capacitor circuit is well suited for use as the source generator for a long resistively loaded mono-cone antenna. A summary of the VPD II pulse generator parameters, both physical and electrical, is given in Table 1.

TABLE 1

VPD II PULSE GENERATOR PARAMETERS

Marx		
1.	Erected series capacity	3.50 nF
2.	Number of stages	65
3.	Output voltage (open circuit nV_o)	6.5 MV maximum
4.	Stage capacity	228 nF
5.	dc charge voltage	100 kV maximum
6.	Stray series inductance	≅ 6.5 μH
7.	Series resistance (stray ≅ 3.5 Ω, lumped 2.5 Ω)	≅ 6 Ω
8.	Insulation	oil
9.	Marx switches	
	• gas type	N_2/SF_6
	• pressure	0 to 30 psig
10.	Marx output voltage range	3:1

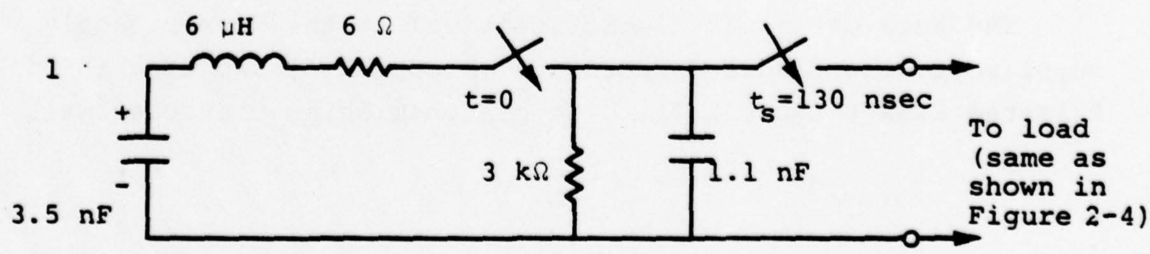

Figure 2-5 VPD II pulser Marx/peaker/load equivalent circuit.

TABLE 1 (cont.)

11.	Marx erection jitter	$\leq$4 ns rms
12.	Marx shunt resistance	$\geq$2.8 kΩ
Peaking Capacitor		
1.	Capacity	1.2 nF
2.	Dielectric	water
3.	Wave impedance	$\cong$6.7Ω
Output Switch		
1.	Gas type	SF_6
2.	Pressure	50 psig maximum
3.	Breakdown voltage variation	$< \pm$ 5%
4.	Breakdown time variation	$< \pm$ 4 ns
5.	Risetime	$<$ 8 ns

2.1 MARX GENERATOR

A 65-stage Marx generator satisfies the system electrical requirements. Erected series capacity is about 3.5 nF and, when taken in parallel with the peaking-capacitor , total generator capacity is about 4.7 nF. Each Marx stage can be dc charged to a maximum of 100 kV ($\pm$ 50 kV with respect to ground). Stage capacity is 228 nF and each stage stores 1.14 kJ at 100 kV, a total stored energy of 74 kJ.

The Marx design is almost identical to the Marx recently supplied to the Sandia Corporation (Figure 2-6) and used in PI's Pulserad 225W (Figure 2-7). The distinguishing characteristic

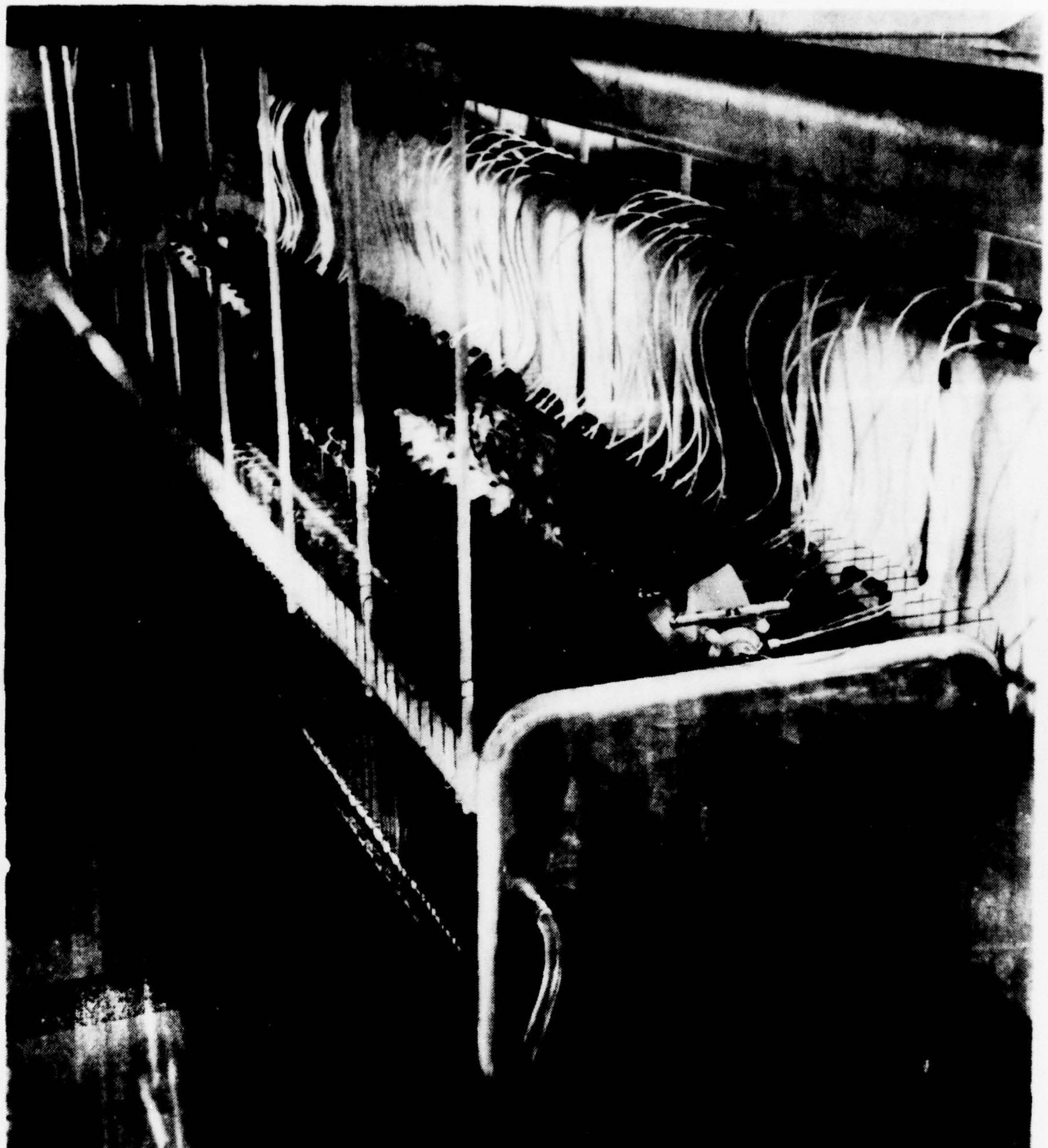

Figure 2-6 Sandia Marx in test tank.

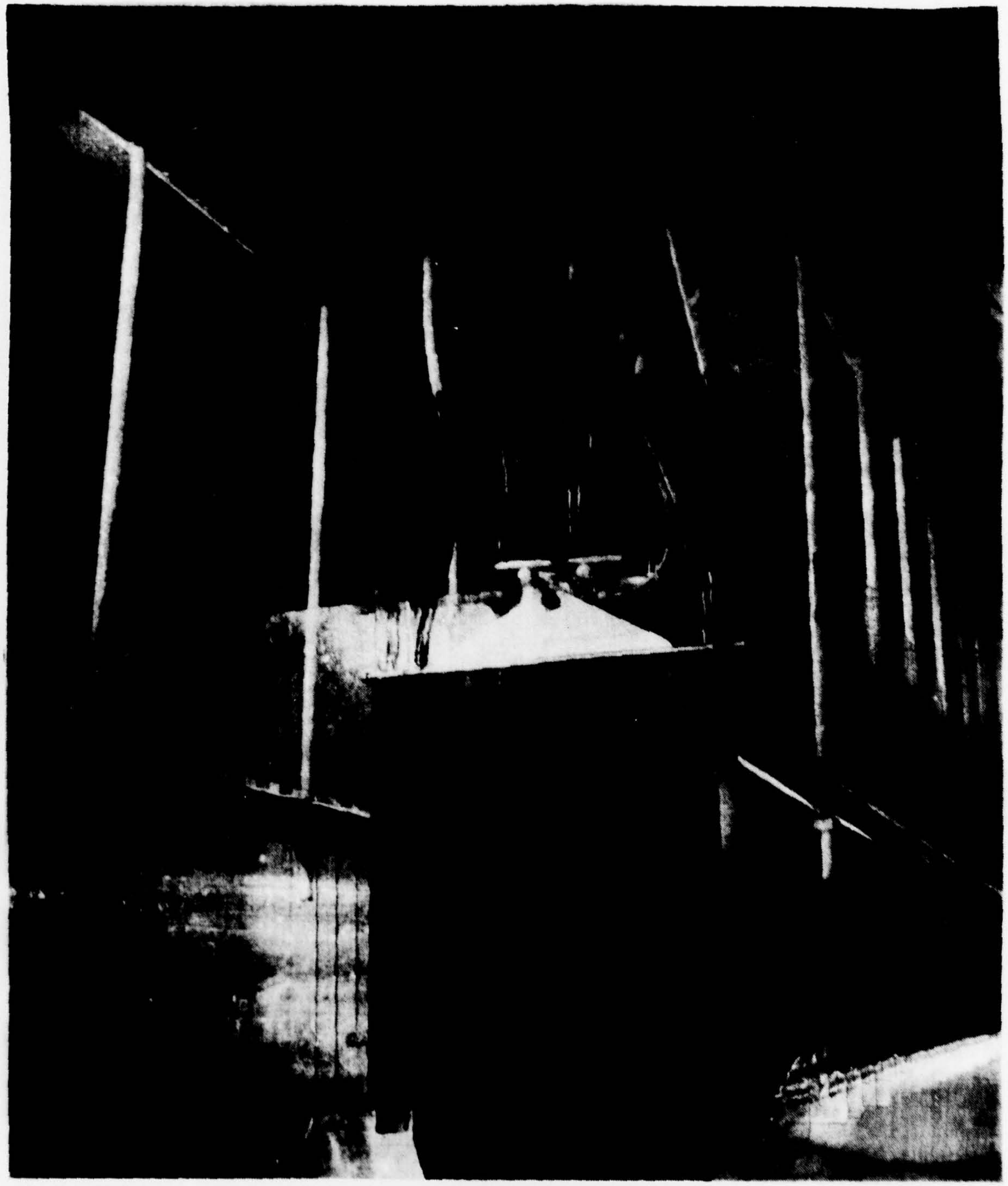

Figure 2-7 Pulserad 225W Marx generator.

of these oil-insulated Marxes is their low inductance modular design, made possible, principally, by the stage energy storage capacitor design. A typical energy storage capacitor is shown in Figure 2-8. Fourteen tubular capacitors are parallel-connected and physically supported on an acrylic sheet. A similar group of capacitors is supported on the other side of the sheet. The halves are electrically connected at their bottom to form a 100-kV "folded" stage. Assembled in this way, Marx stage inductance including the switch and connections is about 100 nH, based upon direct measurement of the 35-stage Sandia Marx in its housing. In addition, Marx equivalent stray series resistance, based upon Sandia Marx measurements, is about 0.06 ohms per stage. Thus, for a 65-stage Marx of this design, stray series inductance and resistance are about 6.5 μH and 3.9 ohms, respectively. However, an additional series resistance is added to limit current and reduce energy storage capacitor reversal in the event of a fault. The total series resistance is about 6 ohms.

The equivalent circuit of the Marx generator is illustrated in Figures 2-9 and 2-10, and the following paragraphs briefly describe Marx components.

2.1.1 Spark Gaps. The Marx generator spark gaps are pressurized gas switches (Figure 2-11) that were originally developed for the Sandia Marx (Figure 2-6). These switches, manufactured and marketed commercially by PI, are rated for 10,000 shots at a peak current of 100 kA and charge transfer of 15 mCb. These switches met the VPD requirements of about 85 kA and 21 mCb, respectively, well within the range of the switch ratings.

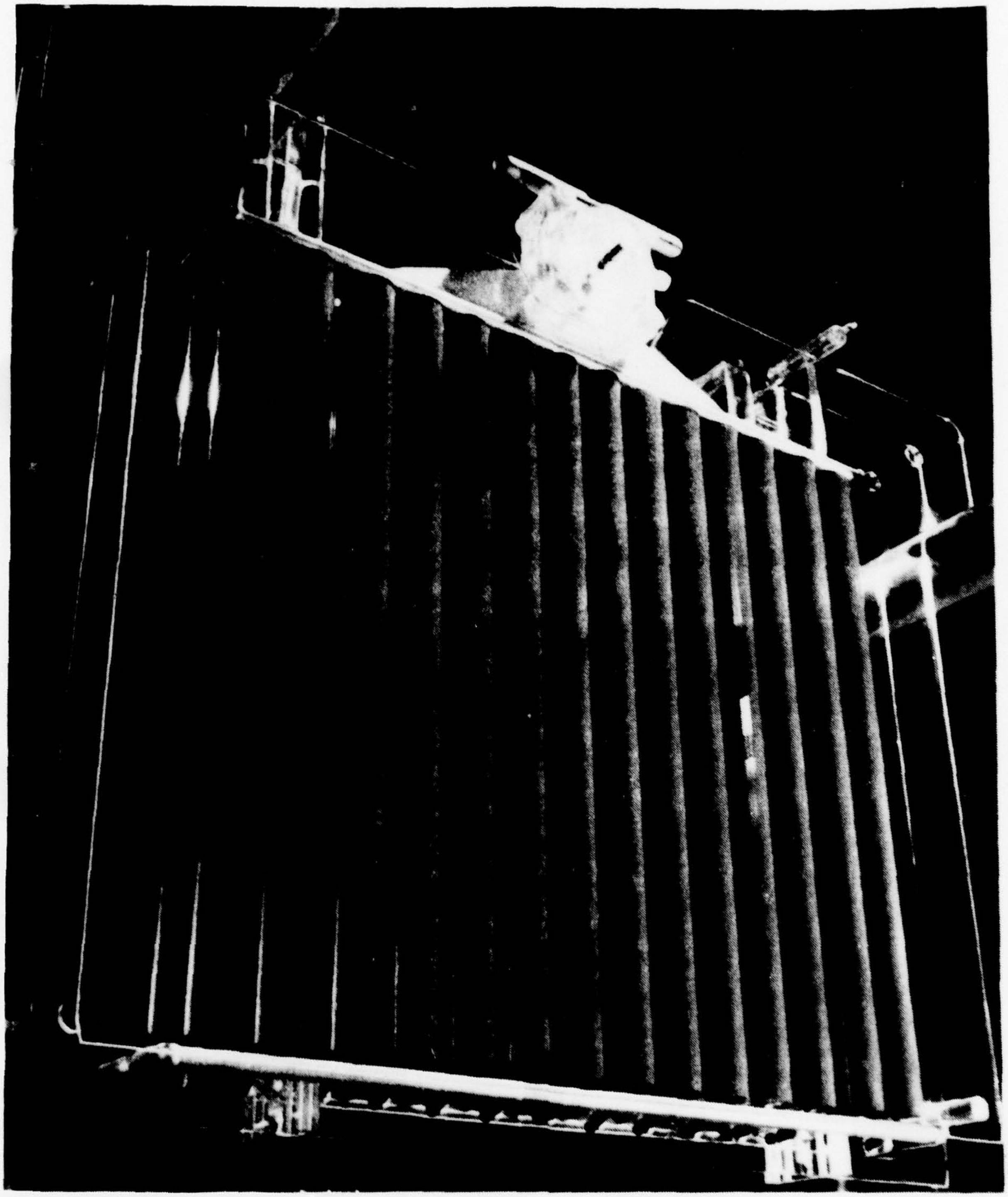

Figure 2-8 Marx generator stage.

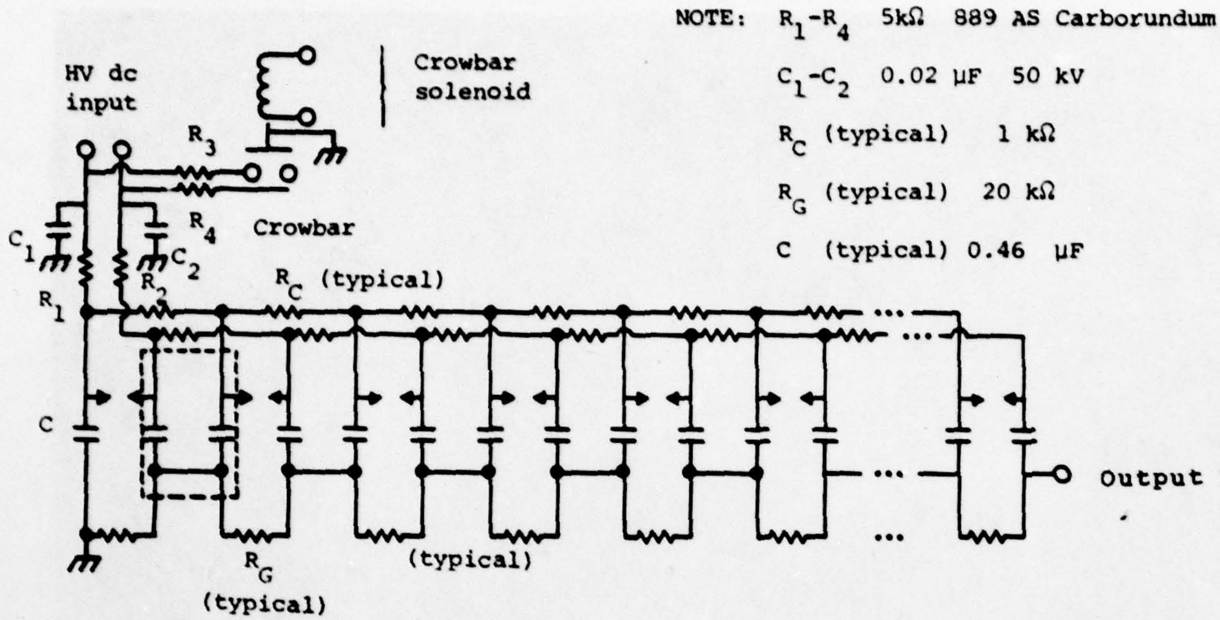

Figure 2-9 Marx electrical circuit (shown without triggering resistors).

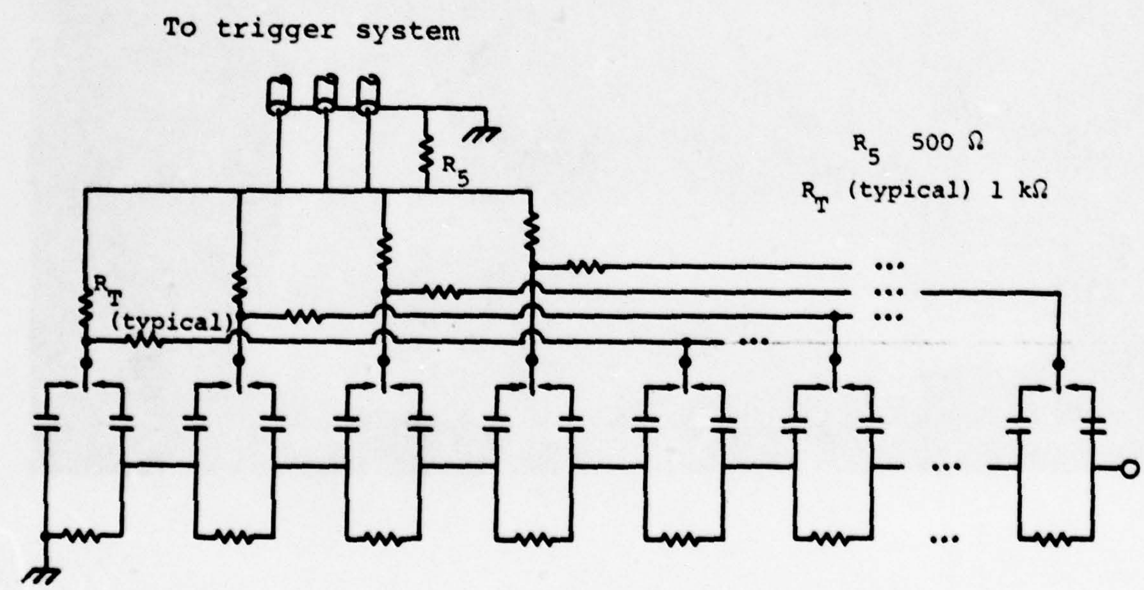

Figure 2-10 Marx electrical circuit (shown without dc charging resistors).

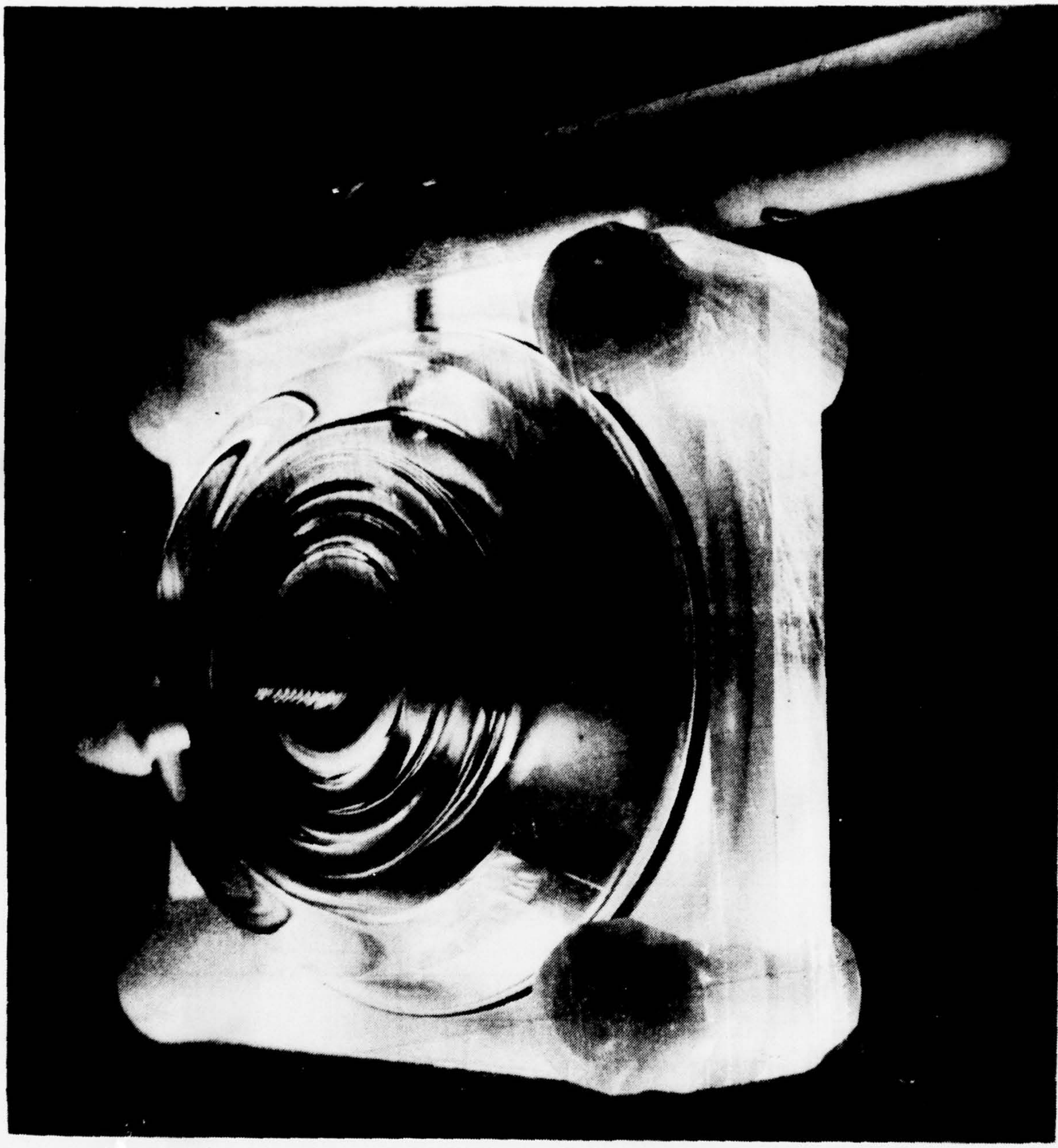

Figure 2-11 Marx generator spark gap.

Spark gap electrodes are fabricated from 1-inch-diameter brass rod stock and gap spacing is about 0.3 inches. Each spark gap is equipped with a midplane trigger electrode that takes the form of an annular brass disk 3/32 inch thick, with a 0.75-inch-diameter hole at its center. The edge of the hole is tapered over a radius of about 0.25 inch to a knife edge with about a 0.01-inch radius. The trigger input and trigger resistive coupling circuit for spark gap triggering is illustrated in Figure 2-10.

These switches are used with both dry air and sulfur hexafluoride (SF_6) at pressures up to about 30 psig to span a dc-charge voltage operating range of 15 kV through 100 kV. However, for the present system Marx erection jitter will limit the operating voltage range with gas pressure and type of gas to 3 to 1, i.e., 33 kV through 100 kV.

2.1.2 Marx Resistors. Principally as a result of the oil-insulated Marx design and the consequent stable temperature environment, Dale high voltage resistors are used in the Marx generator. There are three resistor applications in the Marx as illustrated in Figures 2-9 and 2-10 and each is described in the following paragraphs.

- Charging Resistors. The value for each of the charging resistors is 1 kΩ. The equivalent load placed on the erected Marx by the charging resistors is given approximately by

$$R_{csh} \cong \frac{nR_c}{2} = \frac{65\ (1 \times 10^3)}{2} = 32.5\ \text{k}\Omega$$

and this value in conjunction with a generator capacity of 4.7 nF yields an equivalent e-folding decay time of about 153 μsec.

- "Case-to-Case" Resistors. The electrical location of these resistors is shown in Figure 2-9. The purpose of these resistors is to resistively clamp the capacitor-stage midpoints to ground to ensure balanced charging. In addition, and of equal importance, these resistors are installed for personnel safety since, in the absence of these resistors, capacitor midpoints could assume a potential with respect to ground even if the main capacitor terminals were shorted to ground. The value of each of these resistors is several kilo-ohms and thus, they do not load the erected Marx to any measurable extent compared with the load impedance.

- Trigger Resistors. Each spark gap of the proposed Marx generator is equipped with a midplane trigger electrode. The first four spark gaps are triggered externally and the remaining gaps are resistively coupled (Figure 2-10). Similar resistive coupling is employed in the Sandia Marx. Marx timing jitter is less than 4 ns rms throughout the nearly 3:1 operating range. At the higher operating voltages (> 70 kV dc charge) Marx jitter decreases to less than 2 ns rms.

The triggering resistors form the most significant shunt load on the erected Marx. It can be shown that the effective shunt resistance is given by

$$R_{shunt} \cong \frac{nR_T}{m^2}$$

where R_T is the value of each trigger resistor and m is the extent of trigger coupling, which is m = 4 in this case. Thus, for R_T = 1 kΩ, the proposed value

$$R_{shunt} \cong \frac{65\ (1 \times 10^3)}{16} = 4.1\ k\Omega$$

2.2 PEAKING CAPACITOR

The peaking-capacitor is illustrated in Figure 2-12 and is an unpressurized coaxial water dielectric store. Outer

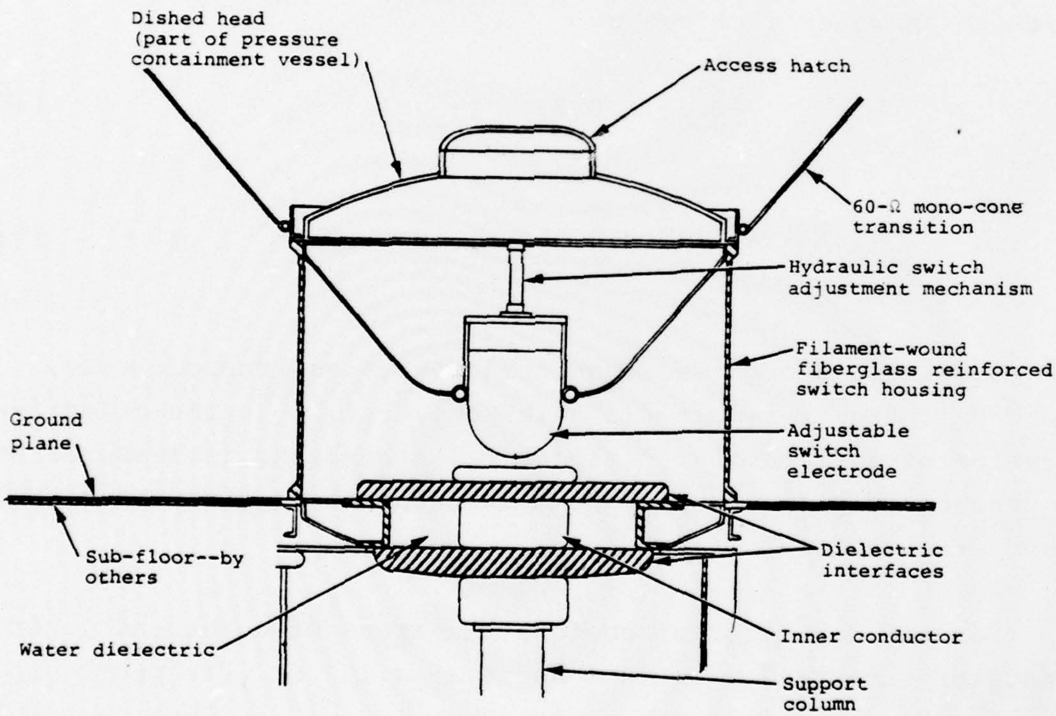

Figure 2-12 Peaking capacitor output switch.

and inner conductor diameters are about 7 feet and 2.58 feet, respectively for the VPD II peaker, and for these dimensions,

peaker wave impedance is about 6.7 ohms. The peaker effective length is about 11 inches, which yields a capacity of 1.2 nF. The shunt resistance for 2.5 MΩ-cm water is about 14 kΩ and in combination with the equivalent shunt resistance of the Marx charging and triggering resistors yield an overall shunt load on the generator of about 2.8 kΩ. Total generator capacity is 4.7 nF; thus the generator open circuit decay time is greater than 13 μs.

The polarity of the water dielectric store is negative with respect to the outer conductor or ground. The breakdown field strength of water is given by

$$\frac{Ft^{1/3}}{A^{-0.06}} = 0.23 \quad (+\ \mathrm{ve}) \tag{1}$$

$$\frac{Ft^{1/3}}{A^{-0.06}} = 0.58 \quad (-\ \mathrm{ve}) \tag{2}$$

for positive and negative conducting surfaces, respectively, where F is the breakdown field (MV/cm), t (μs) is the effective duration of application of electrical stress and is measured at 63 percent of peak stress, and A in Equations 1 and 2 is electrode area in units of cm^2.

For the capacitor dimensions the areas of outer and inner conductors are $18.7 \times 10^3\ cm^2$ and $6.89 \times 10^3\ cm^2$, respectively. From Figure 4b, t is taken to be about 150 ns, neglecting the long low amplitude pulse tail. Thus, for these conditions, the computed breakdown fields for the positive outer conductor and negative inner conductor are 0.240 MV/cm and 0.642 MV/cm, respectively, for normal operating conditions.

Assuming a maximum peaker voltage of 5.5 MV (to compensate for peaker wave impedance), the maximum working stresses in the peaker are 0.052 MV/cm and 0.140 MV/cm for the outer and inner conductors, respectively, and these are about a factor of 4.6 less than the breakdown field.

Normal operating conditions have been assumed for the calculations presented in the previous paragraphs. However, a worst case operating condition is present when the pulser is discharged into a short circuit consisting of a number of conducting straps connected from the mono-cone to ground just outside the mono-cone dielectric enclosure. For this condition, the peaking capacitor "rings" with the inductance formed by the mono-cone and grounding straps. This inductance is estimated to be about 2 μH, if four 2-inch-wide strips are used. The resonant period of oscillation in this case is about 300 ns, which corresponds to a wavelength of about 90 meters. This wavelength is large compared with the electrical length of the mono-cone and as a consequence energy is not effectively radiated from the antenna. The overall result is that the consequent peaking capacitor oscillation is relatively high Q ($\cong$ 10). Calculations indicate that the peaking capacitor voltage reversal is close to 100 percent and damps out slowly, in about 1 μs (e-fold).

In the absence of protective circuitry, the peaking capacitor was designed to sustain full voltage reversal with the center conductor positive with respect to the outer conductor. There is uncertainty regarding the value of t for this condition since "effective time" generally applies to non-oscillatory waveforms. For calculation it is assumed that the waveform is non-oscillatory and damps in 1 μs (e-fold). Thus, t is about 0.45 μs. Using this value and Equation (1) for the center conductor with positive polarity yields a calculated breakdown field of about 0.178 MV/cm, about 27 percent greater than the maximum field at the center conductor for full reversal short circuit conditions.

2.3 OUTPUT SWITCH

The output switch is a high-pressure gas insulated (SF_6) design with a housing length of approximately 4 feet and a diameter of approximately 7 feet. The stress along the envelope housing is about 31 kV/cm. Local field enhancement at the switch ends where attachment is made probably doubles this value; however, the peak stress is less than 72 kV/cm, which is the breakdown field strength of R-12 at 5000 feet above mean sea level.

The switch is a half-symmetry design so that the arc location is close to the virtual mono-cone apex. The switch electrodes are stainless steel and the upper (hydraulically) adjustable electrode is a semi-elliptical head approximately 18 inches in diameter.

The breakdown field strength of SF_6 under conditions where switch voltage is rapidly applied--as it is in this case, in an effective time of about 20 ns--is approximately 120 kV/cm-atm. And thus, for 4.5-atm pressure the breakdown field strength is about 540 kV/cm. Allowing for switch field enhancement, the mean breakdown field is about 360 kV/cm which requires a gap spacing of 15 cm for 5.5-MV peak pulse voltage.

Output pulse risetime is controlled, in part, by stray inductance associated with the output switch and its immediate connections. Arc inductance, for a single channel arc is essentially independent of the current return path because of the small arc diameter and is given approximately by

$$L_{arc} \cong 14\ell \text{ nH}$$

where ℓ is in cm. For ℓ = 15 cm, L_{arc} is about 210 nH. The upper switch electrode branches from the line of the 60-ohm mono-cone and attaches over a distance of about 1-1/2 feet; the associated uncompensated inductance is estimated to be about 90 nH. Total stray inductance is thus about 300 nH, which yields an inductive e-folding risetime ($\tau = L/R$) of about 5 ns. Assuming a pure exponential pulse front, pulse risetime t_r is about 1.4 times the e-fold risetime and for the above conditions is about 7 ns.

In addition to inductive considerations, some finite time is required for switch-arc-channel resistance to decrease to a value which is small compared with load impedance. This is termed the resistive phase risetime given by

$$\tau_R \cong \frac{5\ \rho^{1/2}}{Z^{1/3}\ F_B{}^{4/3}} \text{ nsec (e-fold)}$$

where ρ is gas density in gm/cc, Z is the driven impedance in ohms, and F_B is the mean breakdown field strength in units of MV/cm. For SF_6 at 4.5 atm, $\rho \cong 0.029$ gm/cc, and $F_B \cong 0.36$ MV/cm. Therefore, for Z = 60 ohms,

$$\tau_R \cong \frac{5\ (0.029)^{1/2}}{60^{1/3}\ 0.36^{4/3}} = 0.85 \text{ ns (e-fold)}.$$

Resistive phase risetime is small compared to the inductive rise and thus can be neglected.

Finally, in terms of risetime, consideration must also be given to the conducting geometry which defines the feed point to the mono-cone and the time required for the fields

to establish themselves at the conducting boundaries as a measure of the minimum risetime that can be produced. This phenomenon is often termed the "transit-time" high-frequency response limitation.

The spacing from the ground to the point where the conducting mono-cone becomes uniform and of constant 60-ohm impedance is about 1.7 feet (Figure 2-1). Using a double transit time as a measure of the minimum pulse risetime that can be launched, this spacing corresponds to about 3.5 ns. Thus, it is seen in this case that inductive risetime effects dominate and the resultant output risetime can be expected to be 7 to 8 ns.

2.4 MONO-CONE ANTENNA/ENCLOSURE

The output switch described in the previous section drives the input of a continuous conducting mono-cone. Cone half-angle is 40.4 degrees and the cone apex resides just at the ground plane. Thus, antenna impedance is 60 ohms and is constant over its length from the output switch to its end just outside of the dielectric enclosure (Figure 1).

The dielectric enclosure surrounding the mono-cone contains R-12 (Freon 12) gas to electrically insulate the antenna until the electric fields decrease to a value that can be safely withstood in air. The enclosure dimensions are approximately 17 feet high and 29 feet in diameter.

2.5 CONTROL, MONITORING, AND TRIGGERING SYSTEM

The control, monitoring, and triggering systems consist of the following subassemblies:

- Control Console. The control console contains all controls required to safely control, monitor, and charge and fire the system. The controls are contained within one standard double size equipment rack located at a control point as much as 1000 feet from the pulser.

- Power Supply. The power supply for the system is a standard commercial unit. Balanced charging, i.e., ± 50 kV with respect to ground, is employed to simplify Marx switch trigger coupling. Power supply current is about 36 mA and is sufficient to charge the Marx to 100 kV in about 40 seconds. The high-voltage unit of the power supply is located near the pulser enclosure. A multi-conductor control cable connects the high-voltage unit to the control rack and panel. Standard coaxial cable connects the power supply high-voltage output into the Marx tank via sealed feedthroughs. Marx charging is controlled by a motorized Variac located in the control panel at the remote control point. The Marx is normally charged by manual control of the power supply Variac.

- Trigger System. An adaptation of PI's commercial TG-70 trigger system (Figure 2-13) is proposed to satisfy triggering and timing requirements for the system. Figure 2-14 is a block diagram of the trigger system. As shown in Figure 2-14, the fire command signal is either given manually by way of a pushbutton at the remote control point, or is an electrical signal fed by cable to the control console.

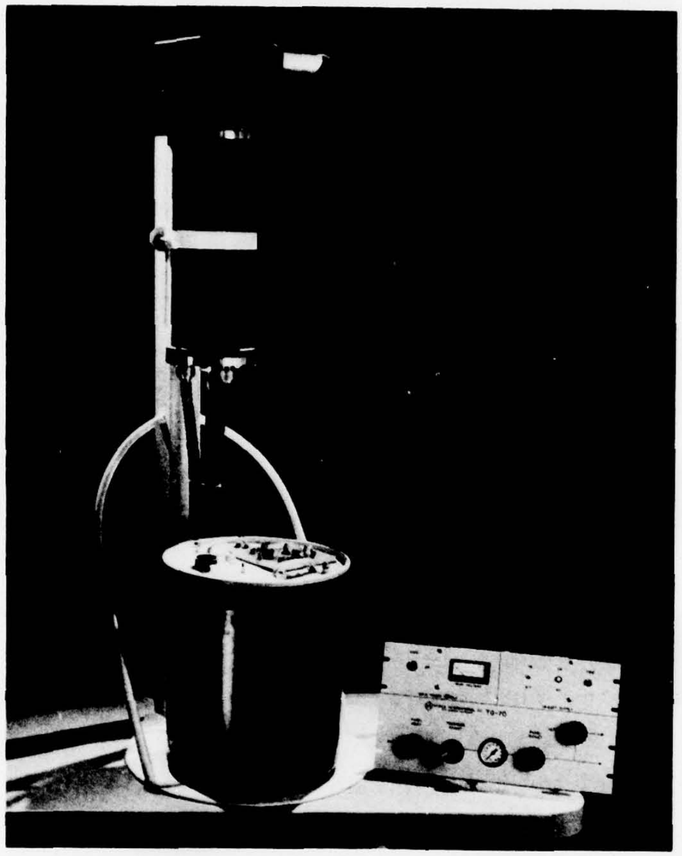

Figure 2-13 TG-70 trigger generator.

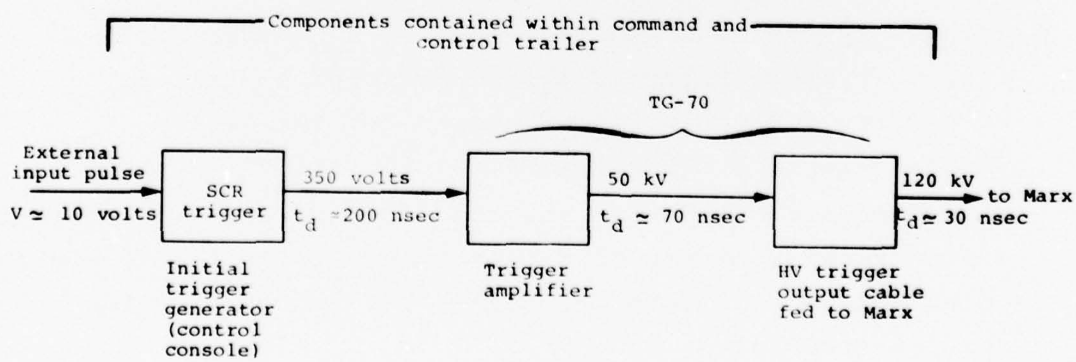

NOTE: Delays noted above are approximate input-output delays excluding connecting cable and final output cables to Marx.

Figure 2-14 Trigger system block diagram.

The first stage of the trigger amplifier is located in the firing chassis at the control console and is a fast SCR circuit which drives a fast-rise 350-volt signal ($\leq$ 5 ns, 10 to 90 percent) into 50 ohms. This signal is fed to the pulser area by means of standard coaxial cable.

The amplifier second stage is a commercially available trigger amplifier available from two vendors. Trigger amplifier output is about a 50-kV fast-rising pulse.

The second stage is coupled to a pressurized-gas spark gap which in turn discharges a low-inductance dc-charged capacitor into two parallel 50-ohm high-voltage output coaxial cables. The output cables are connected via isolating resistors and protective circuitry to the first four Marx-generator spark gaps.

The measured timing jitter of the TG-70 trigger system including the initial SCR stage is less than 2-ns rms. TG-70 output pulse voltage approaches 140-kV and trigger pulse risetime and width are $\leq$ 10 ns and $>$ 100 ns, respectively. The overall jitter of the system, including the Marx and output switch is less than 10 ns rms.

- Pulse Monitoring. The peaking-capacitor described in Section 2.2 will be equipped with a circular flush plate dipole to monitor the peaking-capacitor pulse charge waveform on a shot-to-shot basis. The monitor will be installed in the outer conductor of the peaking-capacitor. Probe output into 50 ohms is a voltage signal proportional to the time rate-of-change of electric flux.

The signal is fed by means of standard 50-ohm coaxial cable to the control area where the signal is integrated and recorded with the use of a standard oscilloscope and camera.

2.6 MECHANICAL SYSTEM DESCRIPTION

The basic pulse generator is composed of the following major components:

1. Marx generator immersed in dielectric oil
2. Dielectric oil tank and storage tank
3. Peaking capacitor
4. Output switch
5. Conical transmission line
6. Dielectric gas enclosure
7. Command and control equipment
8. Charging and power supplies

The Marx or dielectric oil tank is based on designs used by PI for numerous programs.

The Marx generator is supported in the dielectric oil by a series of nylon rods, which in turn are connected to the tank structure. This method of supporting the Marx has been used in all of the PI systems to date.

The mono-cone transmission line is a smooth-surfaced structure fabricated from sheet stock and structural shapes (angles and square tubing). The sheets are riveted to the framework. This construction technique is widely used in the aircraft and sheetmetal industries. Inserts for attachment of the resistive load are provided. These inserts are covered with a plate during normal operation of the pulse generator. A panel is also provided for access to the rear of the output

switch. The mono-cone transmission line is attached to and supported by the outside walls of the gas enclosure. It is estimated that the line weighs approximately 1150 pounds, loading the wall to about 12 pounds per foot. The dielectric gas enclosure is constructed of fiberglass-reinforced plastic. The large cylindrically shaped structure is constructed in segments and bolted together with nonconducting fasteners. Sealing is effected with flat gasket material and taped from the inside surfaces. The roof of the gas enclosure is a segmented dome structure. This type of construction is self-supporting and also provides a volume for the dielectric gas to expand into when daily temperature cycles affect the R-12 gas density.

SECTION 3

FACTORY TEST

3.1 PURPOSE OF FACTORY TEST

The purpose of the factory test was defined in the contract as follows:

> PRELIMINARY TESTING (at contractor's facility): The purpose of these tests is to assure that the pulse generator system is performing satisfactorily before shipment to Kirtland AFB for acceptance testing. In particular, these tests shall demonstrate the performance of: power supplies; the Marx generator; the output switch; the resistive load waveform monitor; the pulse shaping network monitor; and the command and control system in accordance with the Operations Manual, refer to DD Form 1423, A017. These tests are intended to establish that the system can be charged and fired over its design range of operating voltages with ten (10) shots at V_{max} into the resistive load monitor, that the command control and monitoring systems are functioning, to check out the system diagnostics and to gather preliminary data on the system's low frequency performance. The contractor shall prepare a test plan and report the results in accordance with DD Form 1423, A012 and A013. The Air Force project officer or his designee shall observe these tests. Upon satisfactory completion of these tests and with the written agreement of the Air Force, the contractor shall ship the system to Kirtland AFB for final acceptance testing.

3.2 FACTORY TEST PROCEDURE

The test procedure as defined in Physics International Report PITP-900A, dated October 1977, was followed and is quoted here for reference:

> Preliminary factory tests will be performed using a 60-ohm dummy load connection at the output of the pulser from a short section of 60-ohm monocone transmission line to ground. The transmission line will be connected to the output side of the pulser output switch in the same manner as the final configuration of the transmission line within the VPD II facility at the AFWL. For preliminary factory testing, the output switch and resistive load will be housed within a temporary dielectric enclosure containing R-12 gas for electrical insulation.
>
> Preliminary tests are divided into two principal categories: (1) design characteristics and (2) performance characteristics. The following paragraphs describe each of these categories in detail, and specific tests are recommended to demonstrate compliance with system specifications.
>
> • DESIGN CHARACTERISTICS
>
> This portion of the preliminary test is basically a physical inspection of the system with reference to design drawings, component specifications, and to the operation and maintenance manual (preliminary draft) to demonstrate that the high-voltage pulse generator conforms to the statement of work.
>
> Design characteristics applicable to the high voltage pulser are listed in Table 2.

TABLE 2

DESIGN CHARACTERISTICS

1. Electrical Configuration
2. Geometry, Impedance
3. EMP Performance
4. Impedance Discontinuities
5. Pulser/Antenna Interface
6. Pulser Applicability
7. Command, Control and Instrumentation
8. Accessories
9. Power supply and Charging System

Although no specific tests are recommended for the design characteristics listed in Table 2, testing to assess system performance, described in a following section, provides the opportunity to evaluate system design characteristics during operation.

. PERFORMANCE EVALUATION

System performance for factory testing will be evaluated using a 60-ohm dummy load. The load consists of six cupric sulfate-aqueous solution resistors spaced uniformly around a short 60-ohm monocone extension attached to the output switch (Figure 3-1).

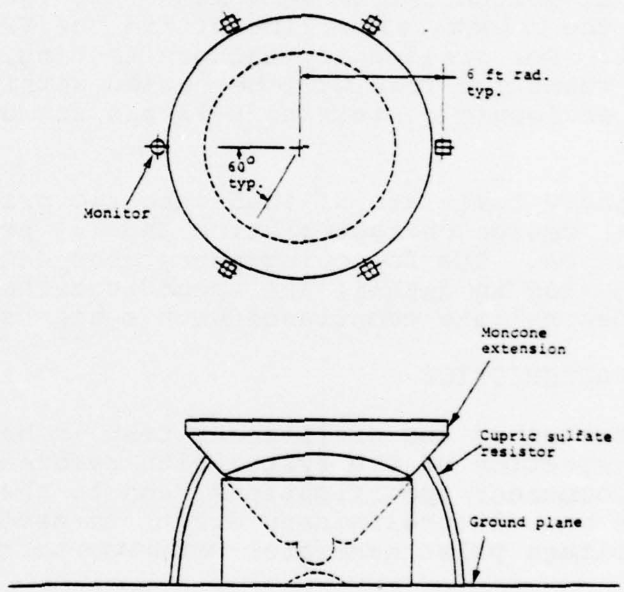

Figure 3-1 Dummy load configuration.

Five system operating performance tests are recommended and the procedures are described in the following paragraphs.

TEST NO. 1: DC CHARGE VOLTAGE

The purpose of Test No. 1 is to confirm the accuracy of the dc-charge voltage monitors throughout the charging voltage range. To accomplish this, the charging connections to the Marx generator will be removed and the Marx will be short circuited to ground. In this way, the measurements can be performed without insulating oil in the Marx tank and without risk of inadvertent Marx erection.

Electrostatic voltmeters with calibration traceable to the National Bureau of Standards will be employed to perform the measurements (more than one instrument will be required to provide the necessary measurement resolution throughout the voltage range). Since dc charging is balanced with respect to ground, two series of measurements are recommended, one for each side of the power supply. The electrostatic voltmeters will first be connected to the positive-polarity charging terminal at the point where connection is normally made to the Marx. The power supply will be energized and the voltage increased in 10-kV steps up to 50 kV. Electrostatic voltmeter readings will be recorded at each nominal 10-kV level. This procedure will be repeated for the negative side of charging circuit.

After completing the described measurements, the recorded values will be compared with the control console dc-charging voltage monitor values and shown to be within the required tolerance ($\pm$ 5 percent). If the measurements reveal unacceptable accuracy, remedial action will be taken to satisfy the required tolerance before proceeding with the remaining tests.

TEST NO. 2: OPEN CIRCUIT TEST

The purpose of this test is to confirm that the open circuit decay time of the pulser is greater than 10 μs (e-fold).

To accomplish the objective of this test, the pulser is charged and fired in a normal manner except that the output switch is adjusted so as not to close, allowing the Marx to "ring" with the water-dielectric peaking capacitor. The voltage waveform across the peaking capacitor is a damped $1 - \cos\omega t$ waveform. The mean output voltage decays with time constant given approximately by the parallel combination of erected series Marx capacity and peaker capacity in parallel with the pulser equivalent shunt resistance.

Because of the "ringing" and long duration waveform applied to the pulser peaking capacitor and from the Marx generator to ground, Test No. 2 will be performed at low output voltage ($\sim$ 1 MV).

The peaking capacitor voltage monitor, a flush-plate dipole capacitive probe, integrated with a passive 1-μs integrator, will be used to measure the resulting waveform. The measured waveform, corrected for frequency response, will show that the system open-circuit decay constant is equal to or greater than 10 μs.

TEST NO. 3: PULSER OPERATION--1/3 V_{max}

For this series of tests, the pulser will be operated in a normal manner producing an output load voltage (negative polarity) of 1.7 MV (nominal). Ten shots will comprise the test. Before beginning the ten-shot series, however, the pulser will be dc-charged to the required voltage and the safety short (crowbar located inside the Marx tank) cycled to demonstrate that the system can be safely discharged without erecting the Marx.

For the ten-shot series of firings, the output waveform monitor associated with the dummy load will be used to assess the output waveform. The waveform will be measured using two oscilloscopes to provide sufficient range in time to assess the overall waveform. Oscilloscope horizontal time base settings will be 5 and 50 ns/division. Both oscilloscopes were triggered from the low voltage pulser command fire signal to determine pulser timing jitter.

The time required to charge and fire the system for each of the ten shots will be recorded.

After the ten firings are completed, the resultant waveforms will be analyzed and the following determinations made:

1. Amplitude

The mean peak amplitude and deviation will be determined from the ten firings and will be shown to satisfy the requirement described in Paragraph 4.2.7 of the SOW.

2. Risetime

The pulse risetime, t_r, will be measured for each of the ten firings, where t_r is defined in Table 3 of the SOW and graphically illustrated in Figure 4 of the SOW. Using the obtained values, the mean risetime and deviation will be determined and shown to satisfy Paragraph 4.2.3 of the SOW.

3. Prepulse

The amplitude and duration of the prepulse will be measured for each of the ten firings and will be shown to satisfy the requirement described in Paragraph 4.2.5 of the SOW.

4. Jitter

To facilitate time jitter measurements, a low-level fiducial pulse will be displayed and recorded with the described dummy load waveform for each of the ten firings. Time delay, measured from a consistent point on the fiducial pulse to the output waveform, will be determined for each of the ten firings. The SOW (Paragraph 4.2.8) specified that the delay be measured from the fiducial pulse to peak amplitude of the output waveform. However, since the time associated with "peak" amplitude may not be sufficiently well defined, Physics International Company recommends that the measurement be made between the fiducial pulse and a consistent point on the rising portion of the output voltage waveform, say, the 50-percent point. Using the measured values of time delay, the time jitter as defined in Table 3 of the SOW, will be determined and shown to satisfy Paragraph 4.2.8 of the SOW.

TEST NO. 4: PULSER OPERATION--2/3 V_{max}

This series of tests is identical to Test No. 3 except that the pulser output load voltage is adjusted to 3.3 MV (nominal).

TEST NO. 5: PULSER OPERATION--V_{max}

This series of tests is identical to Test No. 3 and 4 except that output voltage level is raised to 5 MV (nominal).

After completion of the five tests described in the previous paragraphs the following determinations shall be made:

1. Capacitance

For all 30 waveforms recorded in Test No. 3, 4, and 5, it will be shown, based upon measurement of the pulser output waveform decay time, that the effective value of generator capacity is greater than 4 nF as required by Paragraph 4.3.7 of the SOW.

2. Prefire

Based upon the 30 shots from Test No. 3, 4, and 5, it will be shown that the system satisfied the maximum allowable prefire rate described in Paragraph 4.3.6 of the SOW.

3. Pulse Repetition Rate

Based upon the recorded time required to charge and fire the system from Test No. 3, 4, and 5, it will be shown that the pulser was capable of operating at the rate of one pulse every 2 minutes. The actual pulse repetition rate used in the previously described tests will likely exceed one pulse per two minutes, limited by the time required to obtain and process performance data.

3.3 TESTING CONFIGURATION AND MAJOR COMPONENTS

In accordance with contract requirements the VPD II pulser was assembled at the factory for operation into a dummy load. This dummy load was the terminus of the first section of the conic antenna, which was an integral part of the output switch assembly.

To explore the full voltage range of the pulse generator, a stress relieving profile was mounted on the conic section and the entire switch and conic assembly was enclosed in a temporary housing to retain atmospheric Freon 12 gas. Figure 3-2 shows part of the enclosed output arrangement and Figures 3-3 through 3-10 show the subassemblies of the pulse generator system.

3.4 PRELIMINARY FACTORY TESTS

In the following subsections, the procedures and results of the preliminary factory tests are discussed. The characteristics of the pulse generator, performance into a dummy load, and system modifications are also discussed.

3.4.1 Characteristics of the Pulse Generator. After the assembly of the system and a comprehensive checking of the components and metering circuits, the first tasks were concerned with determining the actual values of the main components of the assembly and estimating those "stray components" that would influence the characteristics of the energy discharge to the load. These determinations were made via two test procedures:

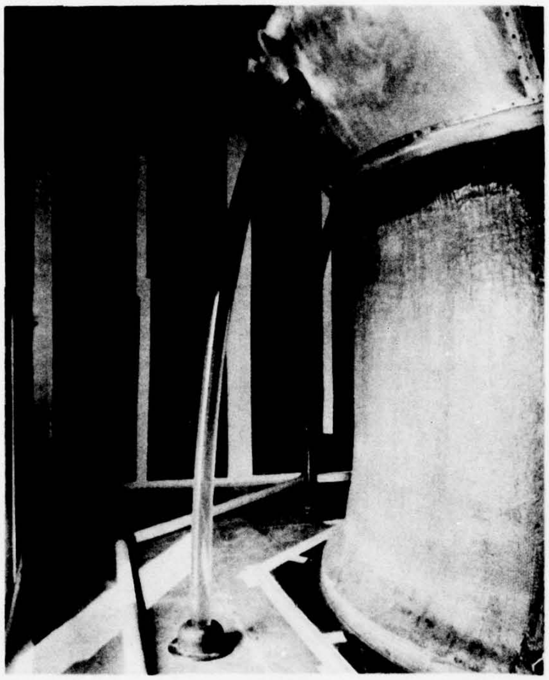

Figure 3-2 Terminated output section in gas enclosure.

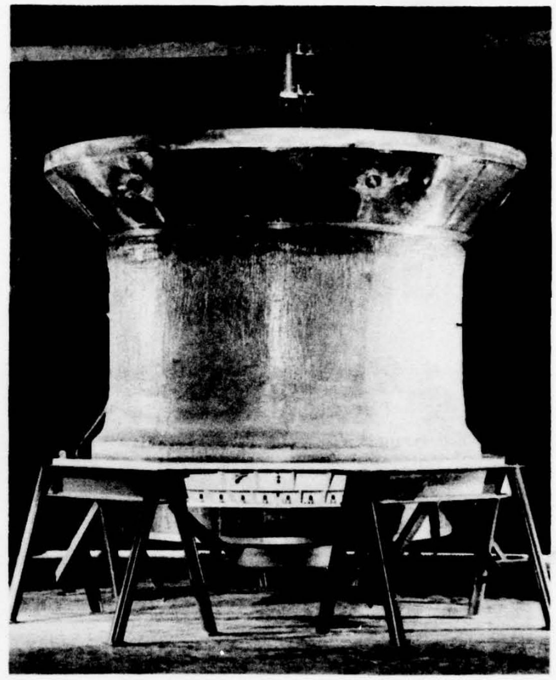

Figure 3-3 Output switch housing mounted on peaking capacitor.

Figure 3-4 Output switch assembly pressure vessel head with switch adjusting actuator.

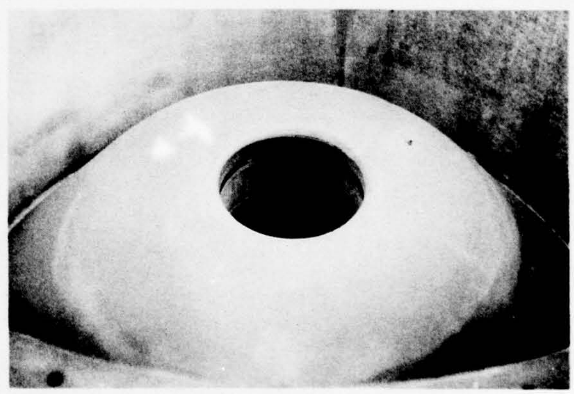

Figure 3-5 Output switch upper conical electrode with adjustable portion removed.

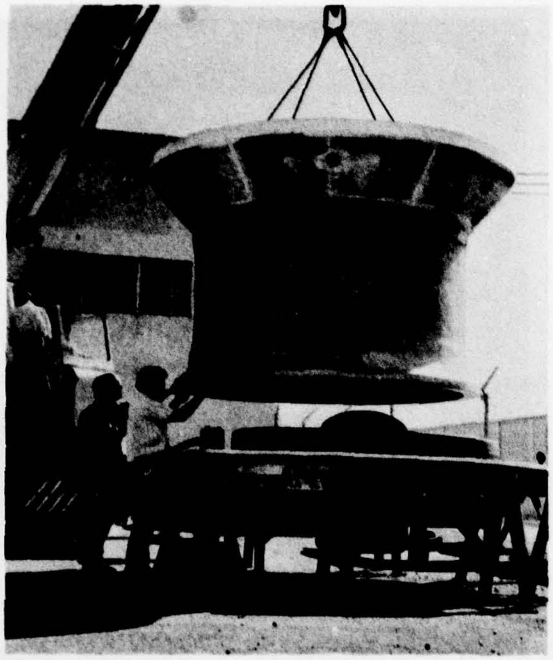

Figure 3-6 Output switch housing lowering onto peaking capacitor.

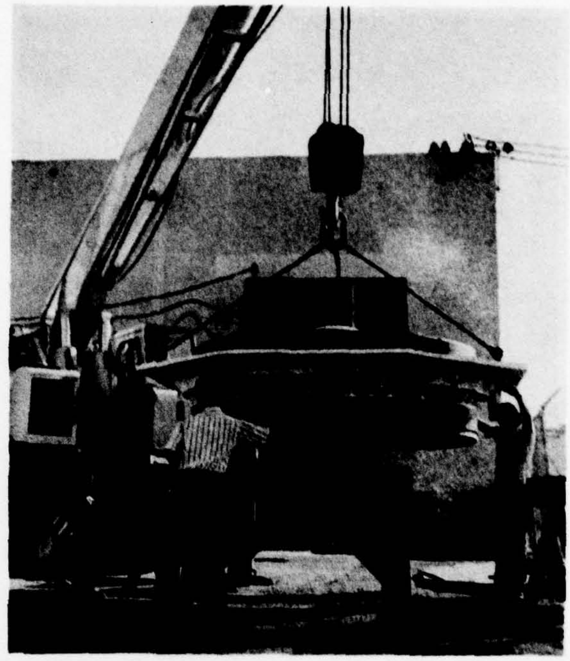

Figure 3-7 Peaking capacitor assembly.

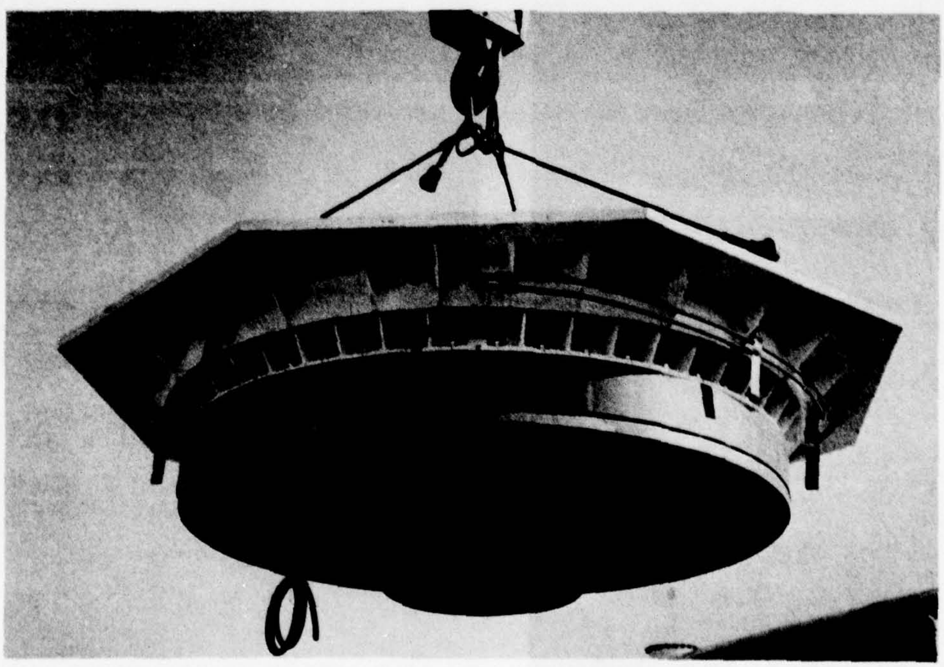

Figure 3-8 Peaking capacitor--oil-water interface.

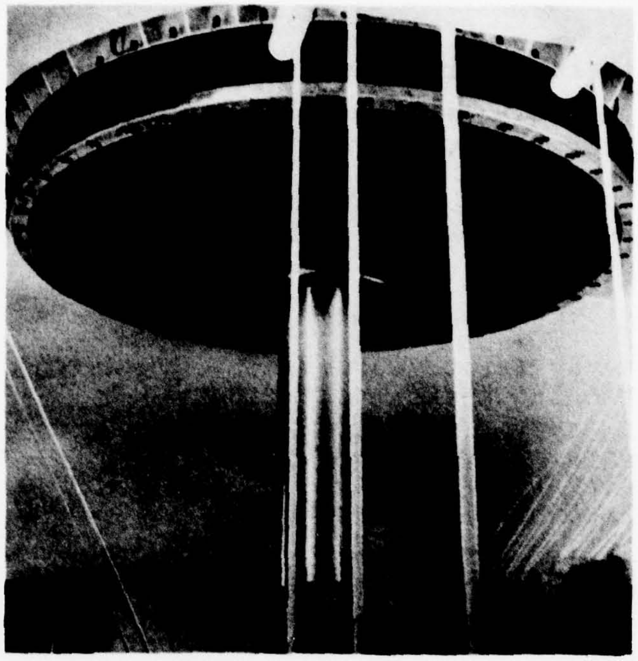

Fiqure 3-9 Junction of Marx and peakinq capacitor.

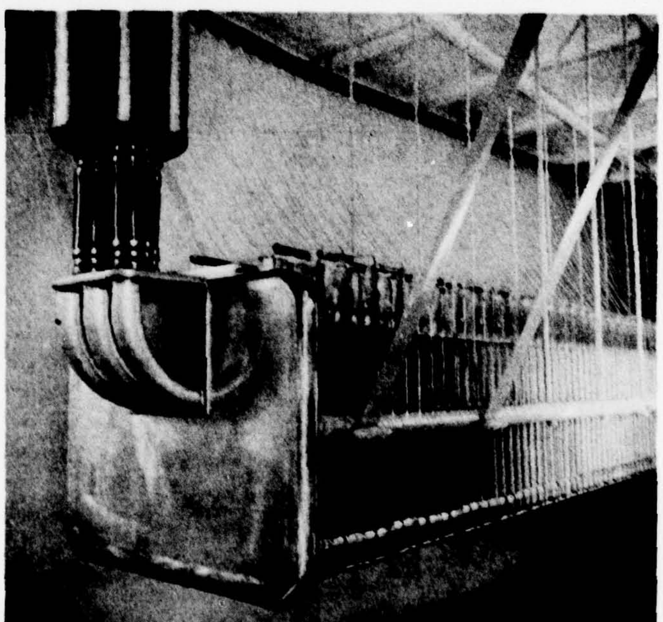

Fiqure 3-10 Marx qenerator--output to peakinq capacitor.

. Marx generator erection into a controlled short circuit

. Marx generator erection into the peaking capacitor without closure of the output switch.

From the analyses of these discharges the following results were obtained:

. Total stray series inductance of Marx and connection to peaking capacitor	7.4 μH
Inductance of connector	0.9 μH
Inductance of Marx	6.5 μH
. Total series resistance	6 ohms
. Average shunt capacitance of Marx stage to ground	9.6 pF
Total effective value to ground	0.21 nF
. Transmission time of Marx as a transmission line in oil (excluding connection to peaking cap)	63.7 ns
. Impedance of equivalent Marx transmission line	102 ohms
. Stray capacitance of connector	0.118 nF
. Capacity of peaking cap + connector + output switch stray + Marx stray	1.95 nF
. Output switch stray	50 pF
. Peaking capacitor value alone	1.55 nF

From these results a simplified equivalent circuit of the pulse generator was evolved, which departs only noticably from the theoretical in the value of the peaking capacitance (Figure 3-11). The shift in peaking circuit impedance was not considered significant (Figure 3-12).

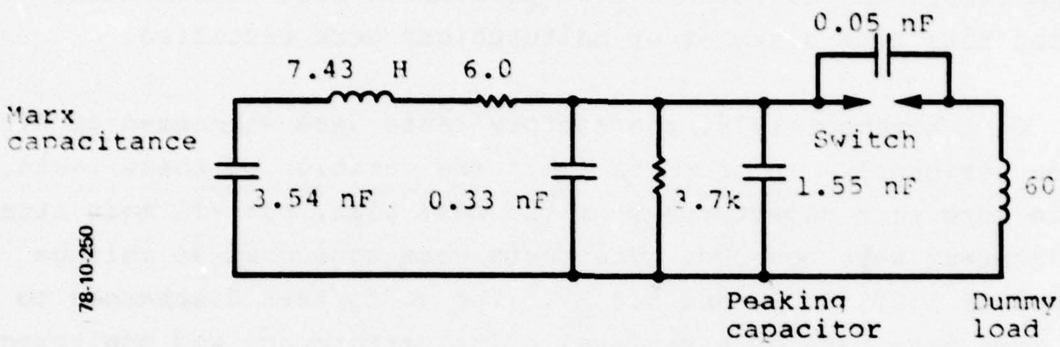

Figure 3-11 Equivalent circuit of pulse generator.

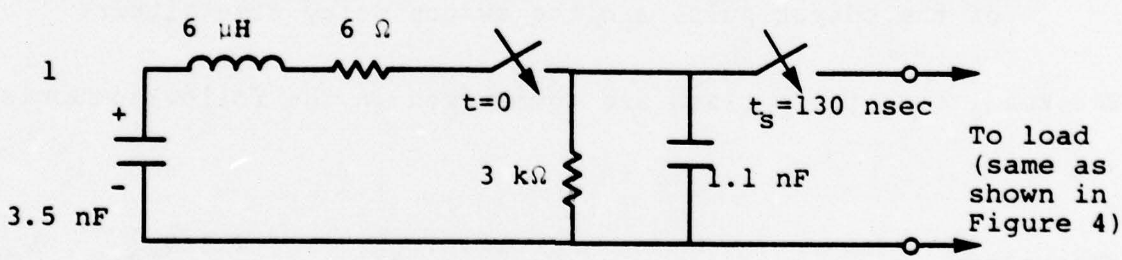

Figure 3-12 VPD II pulser Marx/peaker/load equivalent circuit.

3.4.2 Performance Into Dummy Load. After calibration of monitors and of output switch gas pressure requirements, the pulse generator was operated into the dummy load at increasing peak voltage levels. This operation continued for approximately two weeks before the acceptance test procedures were implemented; during this time a number of malfunctions were rectified.

On 5 November 1976, the factory tests were witnessed by Air Force personnel. In order to limit the duration of these tests, there were some departures from the test plan, but all main items of interest were covered. The tests were conducted at voltage levels of 1.67, 3.33, and 5.0 MV. Ten to fifteen discharges to the load were made at each level. The performance was monitored by these sensors:

. Capacitive probe at the peaking capacitor to measure the peak voltage and time at which the output switch closed.

. Resistive load monitor to measure the peak output voltage and its decay time.

. B-dot sensor in the ground plane to measure the risetime of the output pulse and the switch delay time jitter.

The results of these tests are summarized in the following tabulation:

Parameters	1/3 V_{max}	2/3 V_{max}	V_{max}
Number of Discharges	15	10	14
Number of Prefires	2	--	2
Average Peak Output Volts	1.72 MV	3.21	4.87
Switch Closing Time	200 ns	180	--
Average Decay Time (e-fold)	182 ns	185	--
Average Peak B Field	2.2×10^{3} Tesla	4.1×10^{-3}	5.7×10^{-3}
Peak B Field	0.04×10^{-3} T	0.25×10^{-3}	0.38×10^{-3}
Time to Peak B Field	9.85 ns	8.4	12.67
Time to Peak	1.34 ns	0.81	3.75
Delay Time	54.4 ns	72.7	33.3
Delay Time	--	11.0	10.5

Examples of the monitored performances at 1/3 V, 2/3 V and V_{max} are presented in Figure 3-13.

The following conclusions were drawn by the Air Force Project Officer:

- The performance of the Marx switches in terms of prefire and jitter was marginal and some modifications seemed necessary.
- The RC decay time was less than the specified 240 ns, which could have been caused by the electrical values of the Marx and peaking capacitor.
- The B-field was about 70 percent of the theoretical value with a time to peak of 10 to 12 ns, which indicated that the system was efficient and that the risetime should be less than 10 ns.
- As the voltage increased, the peak fields did not. Additionally, the amplitude jitter and risetime showed increased variability.
- Additional testing was scheduled for May 1977. Examination of the V_{max} discharges shows that dielectric breakdowns occurred in every case. An example of this is given in Figure 3-13.

3.4.3 System Modifications. Following the preliminary factory tests some modifications and refurbishments were necessary before the equipment could be accepted for installation on-site. Upon dismantling the output switch, it was seen that the upper epoxy slab of the peaking capacitor was track marked from the lower switch electrode to the outer edge. Further, the switch fiber-glass housing showed multiple internal tracks. Because the performance of the Marx generator had not been sufficiently stable, it was decided to modify the switch electrode geometries.

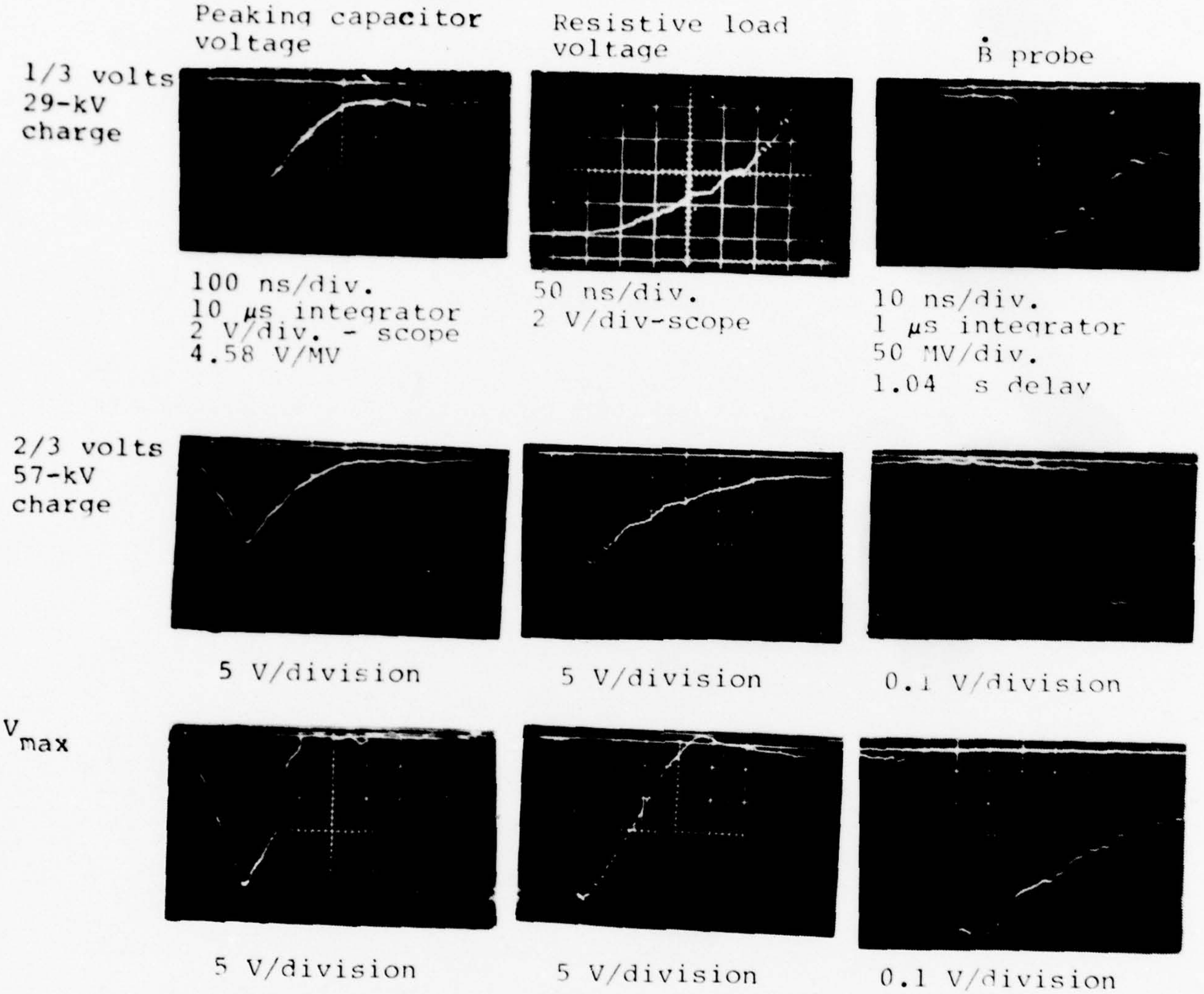

Figure 3-13 Monitored performances.

Marx Generator Switch Modification. To reduce the prefire rate and time delay jitter of the Marx generator the spark gap switches were modified as follows:

- Inter-electrode spacing: increased from 0.75 cm to 1.0 cm
- Diameter trigger electrode orifice: increased from 1.75 cm to 1.91 cm

The performance changes of the generator after these changes were made is shown in Figure 3-14.

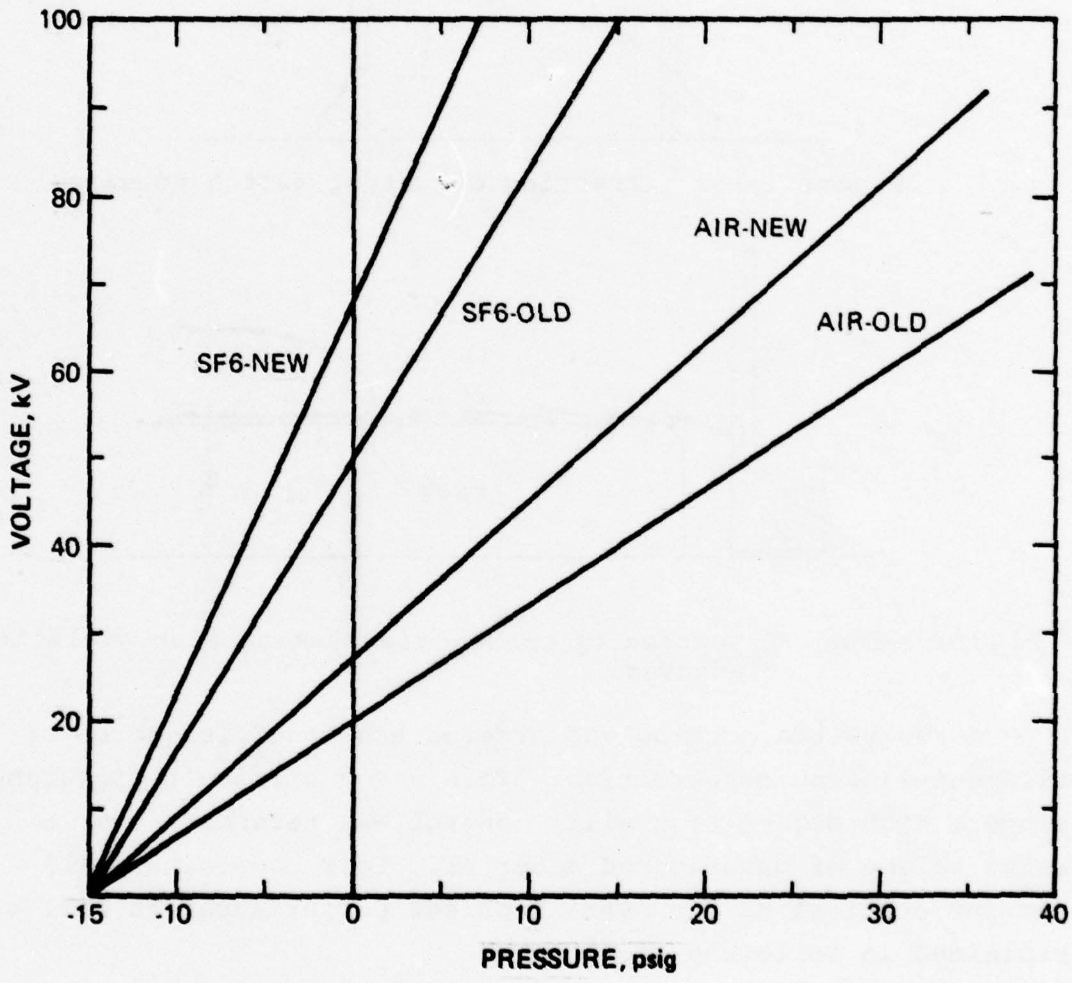

Figure 3-14 Modified performance of Marx spark gap switches.

Modified Construction of Output Switch Housing. The tracking seen on the inner surface and within the material of the switch housing is shown in Figure 3-15a. A number of mechanisms could have caused these dielectric breakdowns, including the growth of discharge sites in faulty material. But one of these destructive processes was likely to be associated with the surface breakdown of the peaking capacitor slab, as shown in Figure 3-15b.

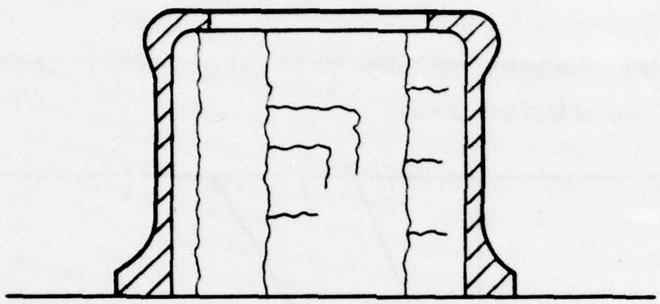

Figure 3-15a Tracking of output switch housing.

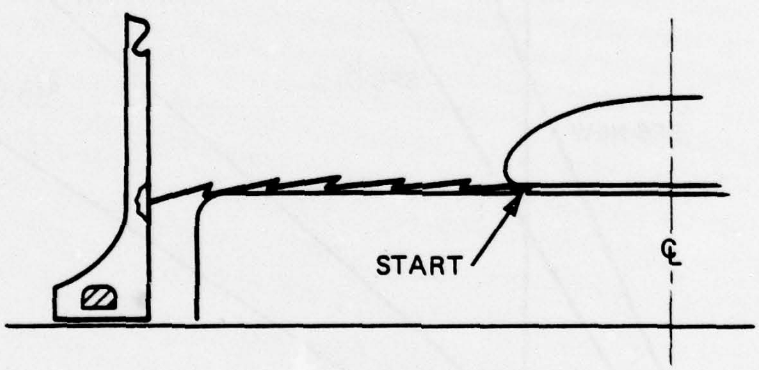

Figure 3-15b Injection of charge via peaking slab dielectric flashover.

A new switch housing was ordered and specified to be of filament-winding construction. This was a difficult procurement since a high degree of quality control was necessary over a large volume of hand-worked material. This component still remains critical to the overall pulser performance, as will be explained in following sections.

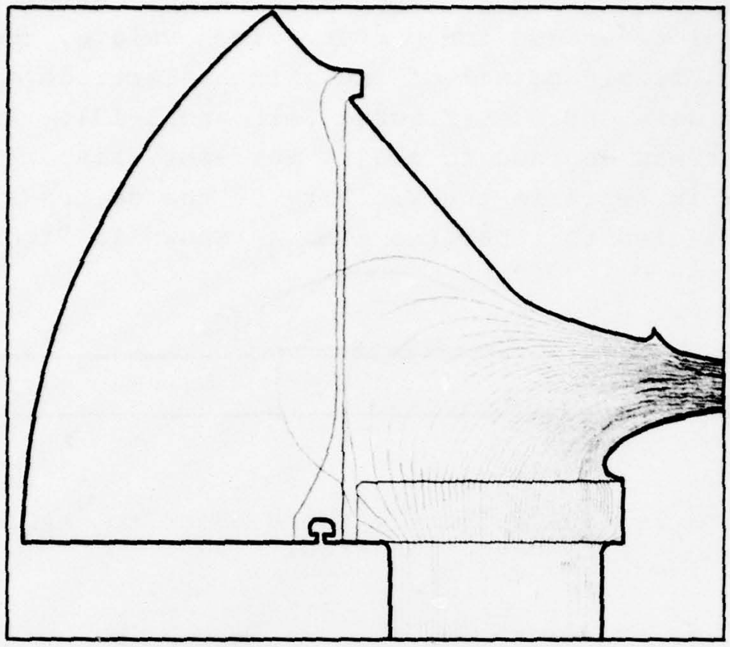

Figure 3-16 Equipotentials original design--open switch.

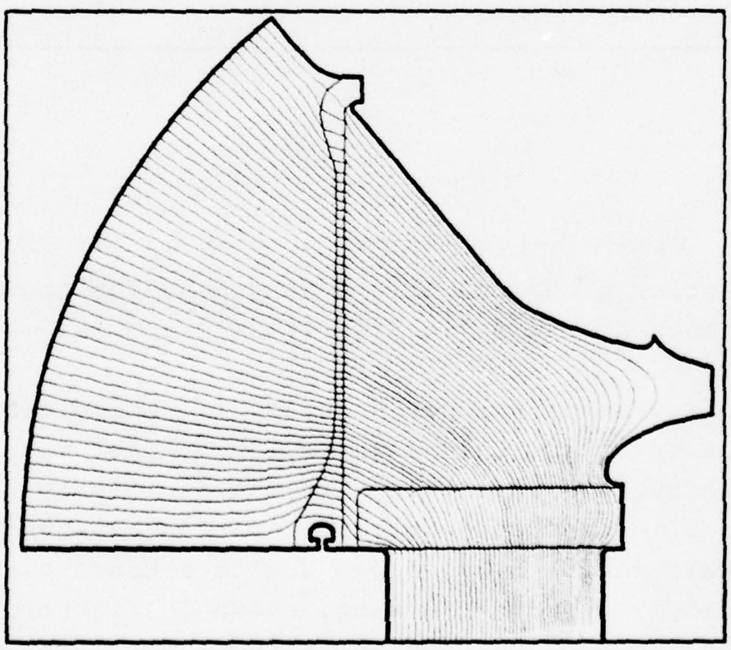

Figure 3-17 Equipotentials original design--closed switch.

Modifications to Peaking Capacitor Slab. After a series of the E-field plots around the output switch volume, the enhancements at the "triple point" of the switch-electrode epoxy-slab air junction were obvious (Figures 3-16 and 3-17). After a PI/AF discussion it was decided to modify the epoxy slab by the addition of a dielectric fence in the vicinity of the switch electrode (Figure 3-18a) and to taper the slab as shown in Figure 3-18b.

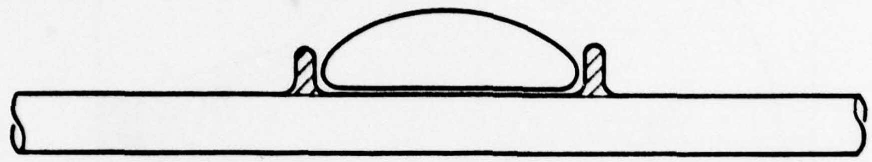

Figure 3-18a Dielectric fence added to peaking capacitor slab.

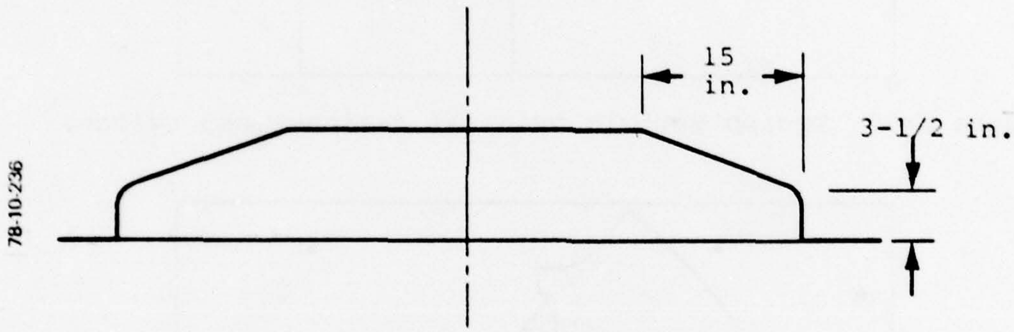

Figure 3-18b Taper of peaking capacitor slab.

The equipotential plots for this arrangement for the switch open and closed cases are shown in Figures 3-19 and 3-20.

This modification was not successful: the dielectric barrier ruptured because of the charge injection. After more field plotting with greater definition, it was decided to look for other configurations. The second design iteration is shown in Figure 3-21. This design also failed due to surface tracking and was superceded by a further design, shown in Figure 3-22. The component was manufactured and installed and remains part of the final configuration.

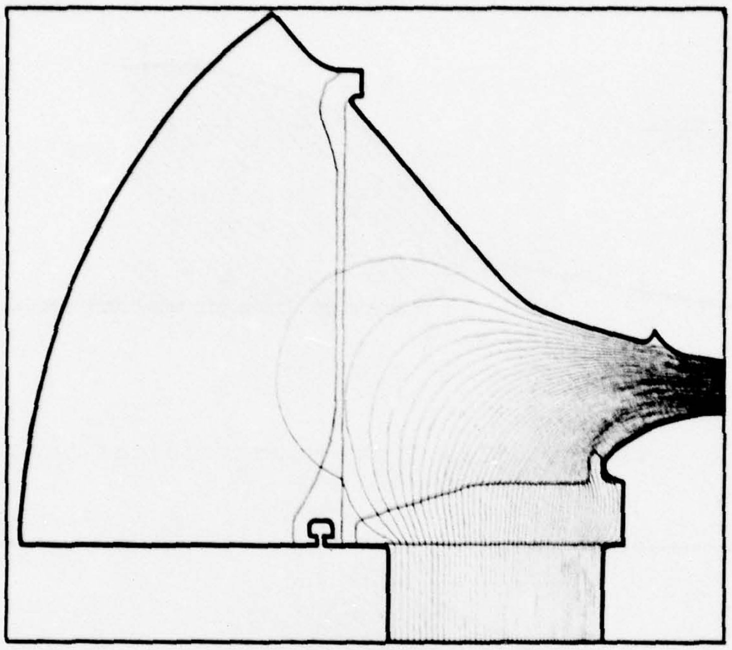

Figure 3-19 Equipotentials--dielectric fence and taper--open switch.

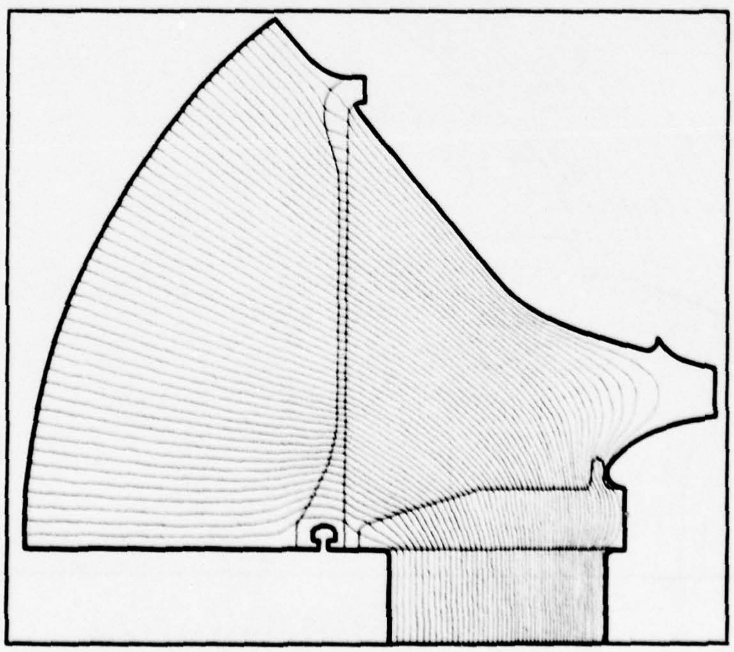

Figure 3-20 Equipotentials--dielectric fence and taper--closed switch.

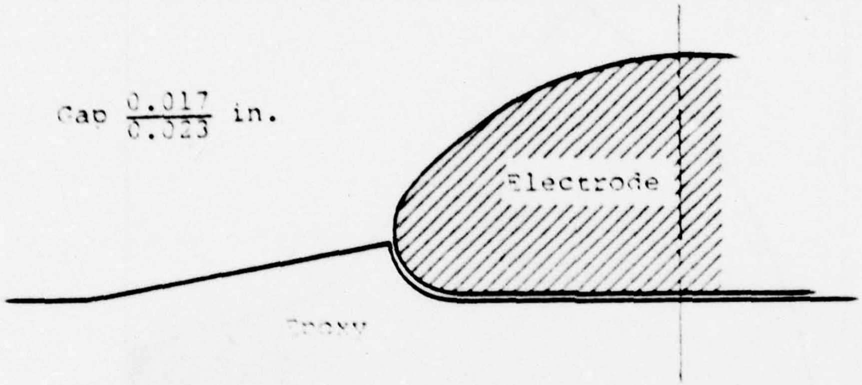

Figure 3-21a Epoxy-electrode-gas junction.

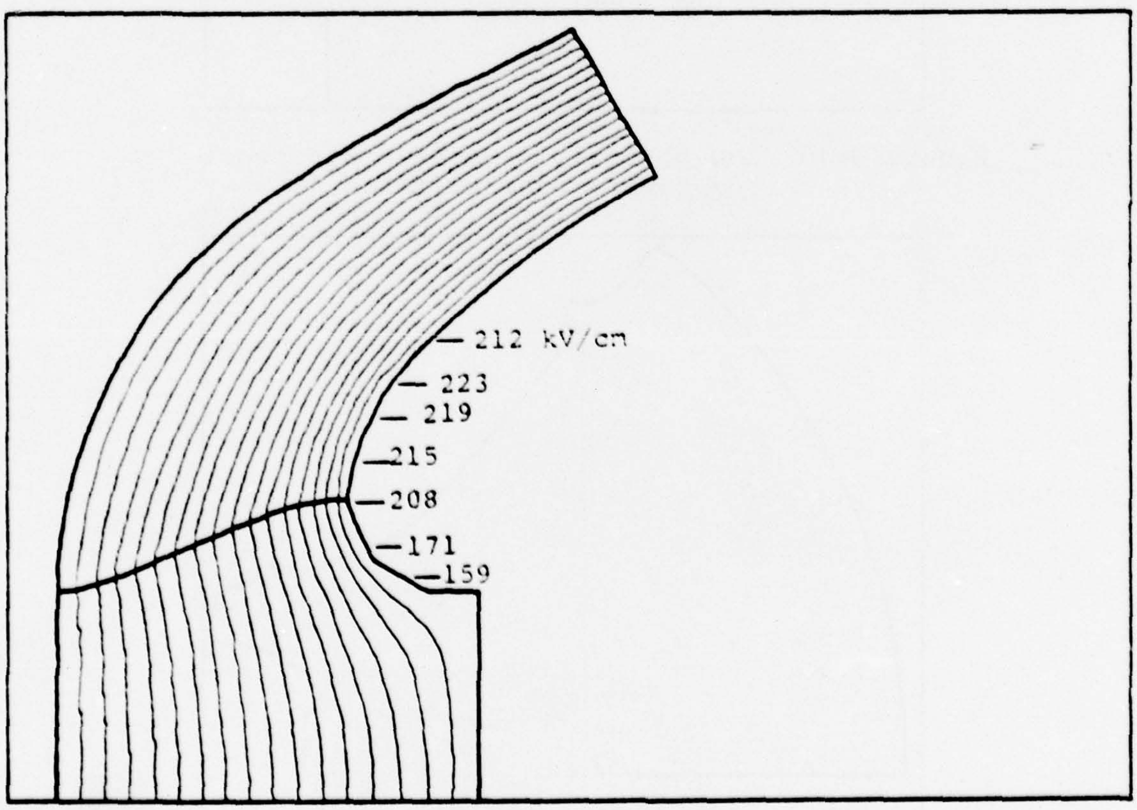

Figure 3-21b Equipotentials.

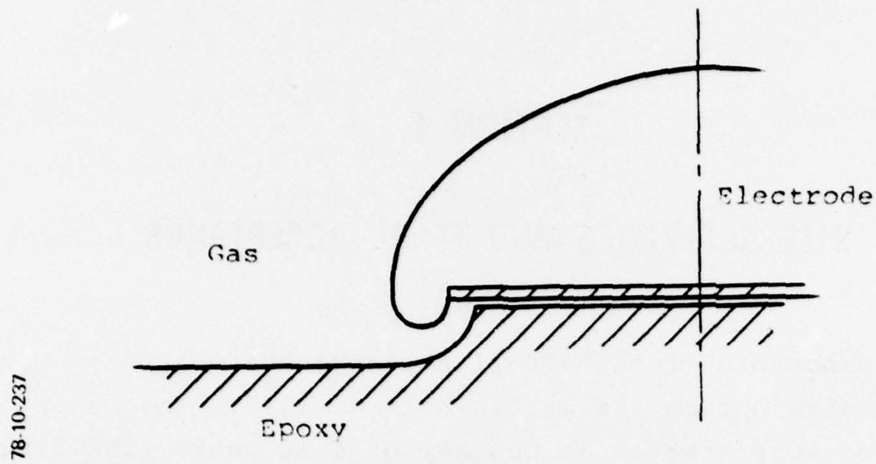

Figure 3-22 Final design of triple-point.

3.4.4 <u>Conclusion of Factory Testing</u>. During these modifications, testing proceeded intermittently. The equipment was transported to the site after the last peaking capacitor slab failure and before the final design was decided upon. Performance up to two-thirds voltage had been satisfactory.

SECTION 4

SITE ACTIVITIES AND FINAL ACCEPTANCE

The components of the VPD-II pulse generator system were shipped to site during the latter half of 1977. The major installation work started in October of that year. The first phase of the testing was to be performed with the dummy load; the load was configured as it was for the factory testing, but capped by a conical section extending to the gas enclosure wall and the antenna interface. Figure 4-1 shows an internal view of the gas enclosure and Figure 4-2 the external view.

At this time, the new output switch housing and the peaking capacitor slab, of final design, were in place.

4.1 PRELIMINARY SITE TESTING

In January 1978 pulse discharge testing began. The monitored peaking capacitor voltage did not display the same low ripple component of the pulse decay which was characteristic of the discharge obtained during the factory testing. The reason was that the second conical section, above the dummy load level, represented a length of unterminated 60-ohm transmission line in parallel with the dummy load. This effect upon the pulse decay can be seen in Figure 4-3.

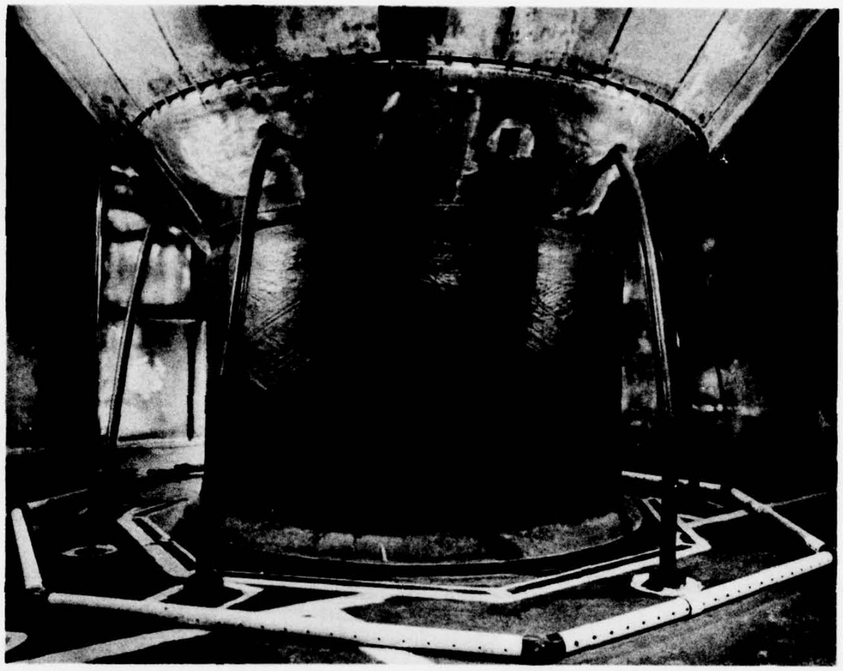

Figure 4-1 Internal view of gas enclosure.

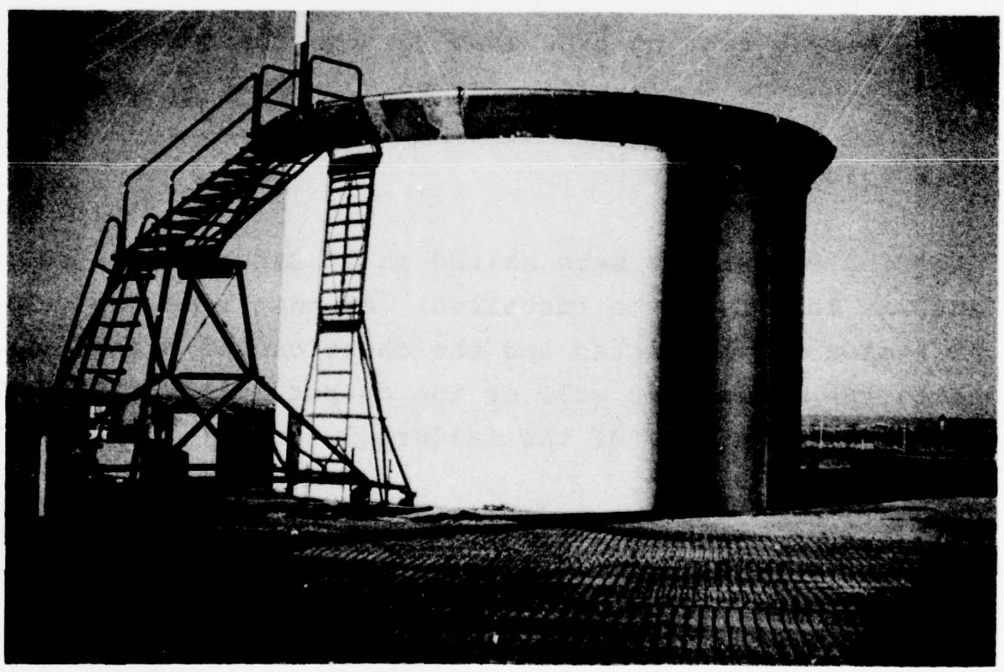

Figure 4-2 External view of gas enclosure.

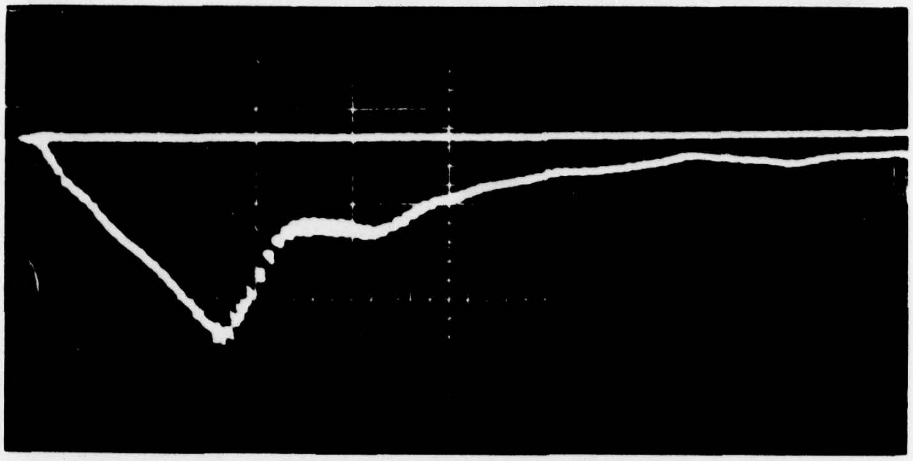

100 ns/division

Figure 4-3 Peaking capacitor voltage.

Preliminary testing proceeded through the 1/3 V_{max}, 2/3 V_{max}, and V_{max} output pulse levels. Beyond the 2/3 V_{max} level there was evidence of dielectric breakdown between 200 and 300 ns after the peak voltage.

Testing operations were halted on 17 January 1978 so that the antenna load could be installed. At that time the output switch region was inspected and the cause of the breakdowns was traced to the dielectric wall of the output switch. Figures 4-4 and 4-5 show the nature of the failure.

After inspection of the failure, it was decided that the electrical stresses must be relieved at the base of the housing where the probability of potential breakdown areas was high.

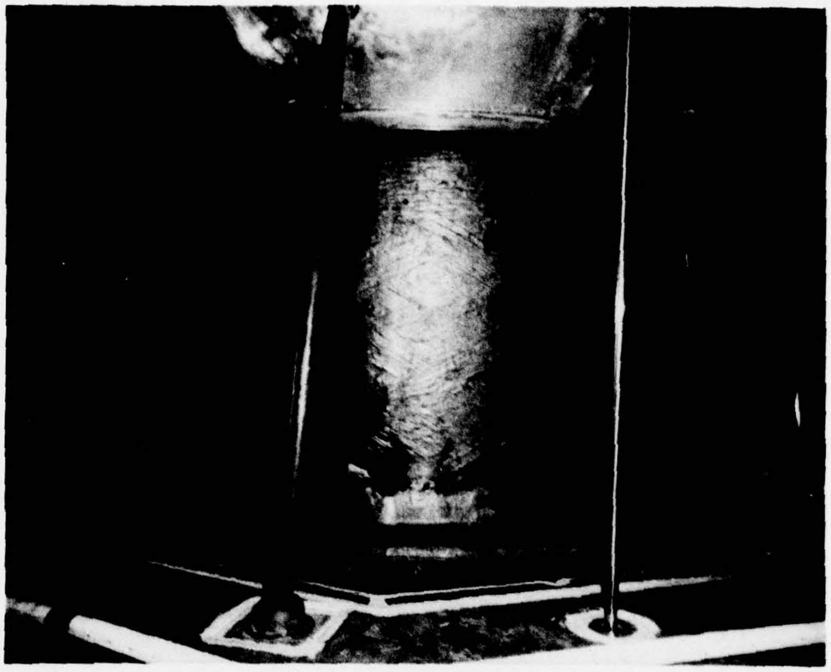

Figure 4-4 Region of output switch breakdown.

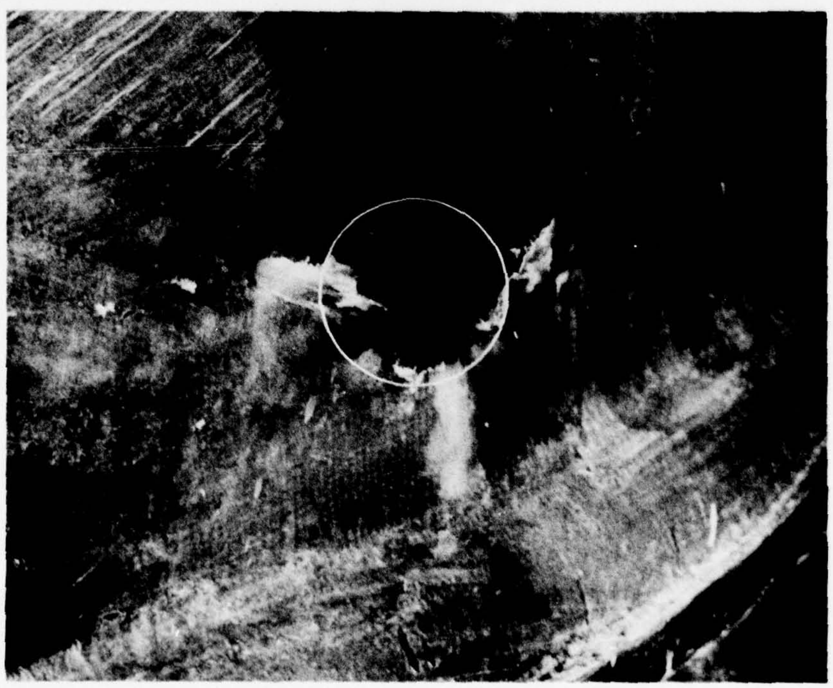

Figure 4-5 Region of output switch breakdown (closeup).

Figure 4-6 illustrates the electric field distribution after switch closure and the direction of the dielectric failure is indicated.

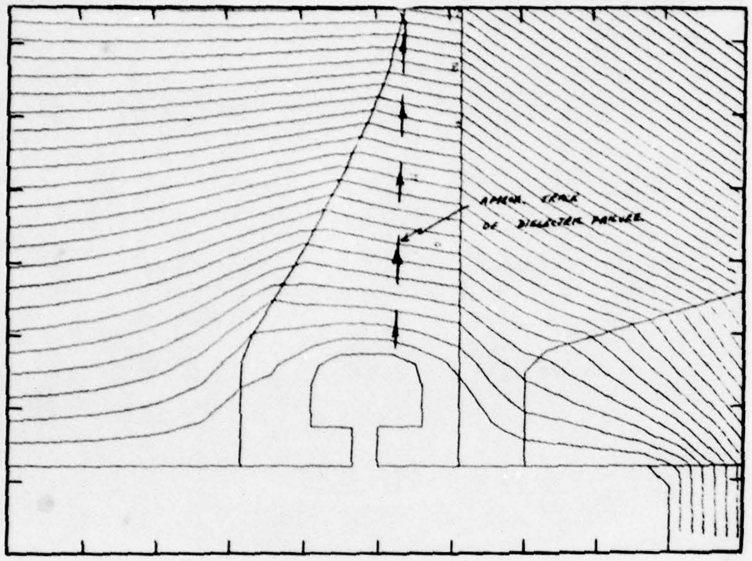

78-10-247

Figure 4-6 VPD switched equipotential plot.

After several trial geometries were examined, the stress relieving ring geometry of Figure 4-7 was chosen.

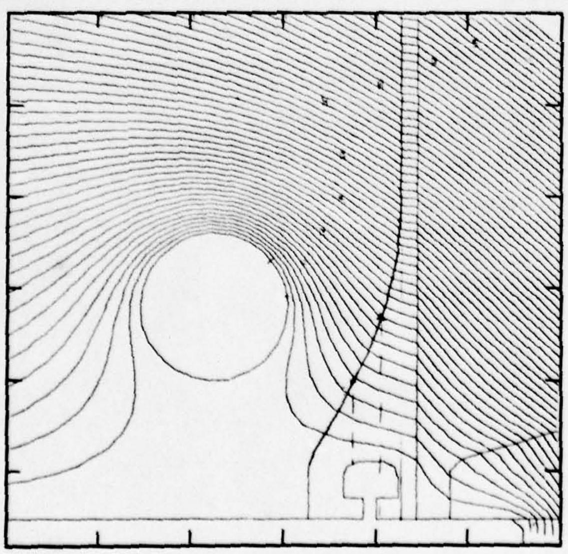

78-10-249

Figure 4-7 Equipotential plot showing VPD 8-inch ring with 5-inch gap.

This gave significant protection to the vessel with a peak stress at the ring surface of 83 kV/cm--a stress level that had been supported in one atmosphere (5000 feet) SF_6 at the time of the ALEC installation. This ring was fabricated in four sections for convenience of installation. Meanwhile, the spare switch housing was installed and the damaged housing was repaired.

Following the switch housing replacement and before the installation of the ring, the pulser was operated into the full antenna system at a reduced voltage on 31 March 1978. There were no breakdowns.

With the antenna loading, the pulse decay time extended into the microsecond range and it was apparent that the electrical stresses would be more severe than for the dummy load conditions. Typical peaking capacitor voltages for the antenna load are shown in Figure 4-8.

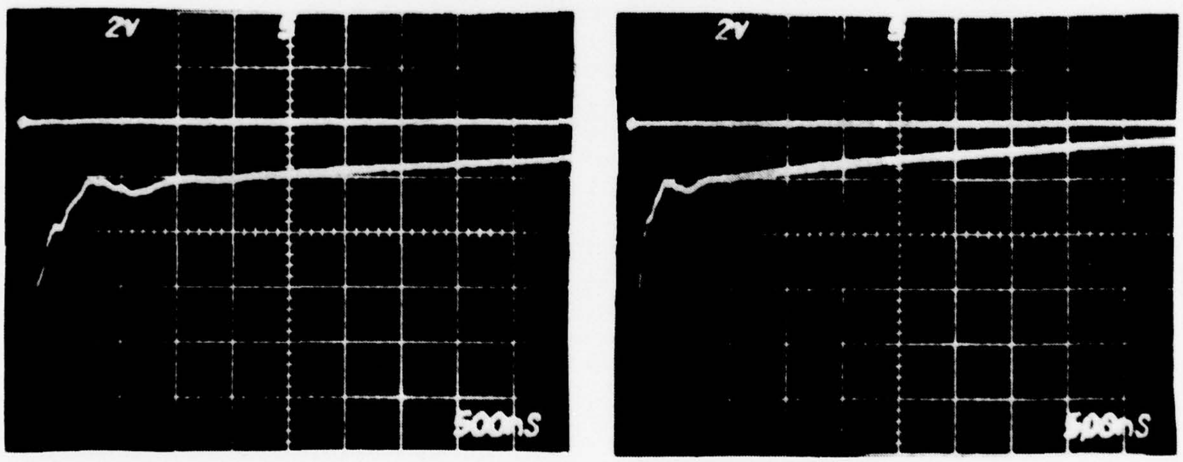

500 ns/div. 1.0 μs/div.

Figure 4-8 Main antenna load, peaking capacitor voltage.

Following these low level tests, the protective ring was installed on 12 April 1978 in preparation for the final acceptance tests scheduled for 18 April 1978.

4.2 FINAL ACCEPTANCE TESTS

The basis for these tests was derived from the A.F. Statement of Work, Reference FY 3592-75-10182-00 March 1975 (Revised), Section 4.9. The relevant subsection is quoted here in full for reference. The pertinent figures from the statement of work are also included.

> 4.9.2 FINAL ACCEPTANCE TESTING (at Kirtland AFB): The final acceptance test of the pulse generator system shall take place in the upgraded Vertically Polarized Dipole (VPD II) EMP simulator at Kirtland AFB, New Mexico. The contractor shall furnish the pulse generator system, supplies, engineers and technicians necessary to install, service and operate the pulse generator system until completion of final acceptance testing. The contractor shall prepare a test plan/procedures and report the results in accordance with DD Form 1423, A012 and A013. The contractor shall perform data analysis necessary to demonstrate that the pulser specifications have been satisfied. There shall be several different types of test performed during the final acceptance testing. The types of test and the pulser characteristics they are intended to confirm are listed in the following paragraphs. All the data taken during the acceptance testing will be corrected for the effect of the measurement system. The sensor, cable, integrator and oscilloscope response will be removed from the measured data by deconvolution or frequency domain correction. For the purpose of acceptance testing a successful shot shall be defined as occurring when the pulse generator has been charged to the selected voltage level, fired on command and a resolvable data trace acquired. Sensors, oscilloscopes, cameras, shielded data collection spaces (screen room) and interconnecting cables shall be GFE to the contractor during final acceptance testing. The contractor shall supply a GFE list with the Facilities Requirement Plan, A007.

4.9.2.1 Operational Testing: This series of tests is intended to establish that the pulse generator system satisfies certain general operational requirements such as repetition rate and RFI/EMI. These tests shall be conducted after the pulser is installed in the VPD II facility and the antenna attached. They will include:

4.9.2.1.1 Command and Control (C&C): All C&C functions and monitors shall be operated and checked in accordance with the Operation Manual, refer to DD Form 1423, A017. Reference paragraph 4.6.

4.9.2.1.2 The pulser shall be capable of operating at full voltage into a resistively loaded conical antenna with no resistive connection between the antenna and ground.

4.9.2.1.3 Peak Voltage and Prefire: The pulser shall be operated across its entire range at three different voltage (1/3 V_{max}, 2/3 V_{max}, and V_{max}) settings. A series of twenty (20) shots shall be fired at each setting. The peak voltage (refer to paragraph 4.3.2) and prefire (refer to paragraph 4.3.6) shall be measured for each series of shots.

4.9.2.1.4 Field Uniformity: Two field sensors shall be located at a fixed range, to be determined by the contractor, which has sufficient clear time to allow for observation of the peak amplitude of the radiated pulse before arrival of reflections from the antenna structure. The generator shall be fired at maximum output voltage for a series of ten (10) shots. One sensor shall act as a reference data point during the series. The other sensor shall be rotated at a fixed radius (as defined above) around the pulser, moving thirty-six degrees (36°) between each shot. After each shot the data shall be compared and the variance in peak amplitude shall be less than plus or minus five percent ($\pm$ 5%). Refer to paragraph 4.2.6.

4.9.2.1.5 Short Circuit: The pulser shall be fired three times into a short circuit at maximum output voltage.

4.9.2.1.6 Open Circuit: The pulser shall have an open circuit decay constant of not less than 10 microseconds (10 μsec). This shall be demonstrated by firing the pulser into an open circuit at 1/3 V_{max} (nominal).

4.9.2.1.7 Pulse Repetition Rate: The contractor shall demonstrate that the specification in paragraph 4.3.3 has been met.

4.9.2.1.8 Safety Gaps: If the pulser is equipped with protective gaps to prevent damage to peaking capacitors or other pulser components due to malfunction, the gaps will be such that they do not operate during normal pulser discharge into the VPD II antenna.

4.9.2.2 High Frequency Testing: The purpose of this series of tests is to determine the early time characteristics of the pulse generator system. The basic test concept is to record the early time fields at various ranges from the pulser. Both derivative and integrated data shall be taken. The measurements shall be made with the pulse generator installed in the VPD II simulator. The instrumentation shall consist of ground plane mounted B-Dot and D-Dot field sensors coaxial cables, passive integrators and high frequency, real time oscilloscopes. The intent is to position at least one measurement point such that there is sufficient clear time to observe the risefront of the signal from the start of the main output pulse t_1 to the peak t_p. A typical sensor location would be at a horizontal range of 5 meters from the main output switch. This measurement location would be used to determine the following parameters of the early time output waveform based on fifty (50) successful shots at maximum output voltage.

4.9.2.2.1 Peak Amplitude: Peak amplitude shall be determined based upon the measured peak Er product.

4.9.2.2.2 Amplitude Variation: The average amplitude shall be calculated and the rms deviation shall be less than plus or minus five percent ($\pm$ 5%). Reference paragraph 4.2.7.

4.9.2.2.3 Risetime: The risetime shall be determined based on the average of fifty shots using the formula given in Table 3.

4.9.2.2.4 Risetime Repeatability: The maximum deviation of the risetime based on the average risetime established above shall be plus or minus one nanosecond ($\pm$ 1 ns) or less.

4.9.2.2.5 Inflections: It is desired that the risefront of the waveform from t_1 to t_2 be smooth and free of "steps" or "knees." These correspond to changes in slope or dv/dt. The presence of inflections on the risefront will be determined by analysis of B-Dot and D-Dot data.

4.9.2.2.6 Prepulse: The prepulse is defined as the portion of the signal which occurs prior to the firing of the output switch at t_f. On Figure 4 t_f is defined as the intersection of the base line and a line defined by the points (E_2, t_2) and (E_1, t_1) on the risefront of the wave. The points (E_2, t_2) and (E_1, t_1) are arbitrary and are used in defining risetime (t_r). This signal is caused by the charging current during buildup of voltage across distributed peaking capacitors. The duration of this signal is generally from fifty to two hundred nanoseconds (50 to 200 ns). The prepulse will be measured at the close-in measurement location and defined as the maximum instantaneous field strength prior to firing of the output switch. Reference Table 3.

4.9.2.2.7 Jitter: Jitter is defined as the variation in the time interval between any low level fiducial pulse (t_{ref}) of the overall pulse generator and the peak amplitude of the radiated waveform (t_p). It should be noted that the low voltage signal referred to above is one present in the pulser trigger generator, and does not include the link between the pulser control console and the trigger generator. Therefore, the jitter will be measured by computing root mean square value of $t_p - t_{ref}$ for fifty (50) successful shots.

4.9.2.3 Low Frequency Testing: The purpose of this series of tests is to determine the intermediate and low frequency response characteristics of the pulse generator system. The pulser will be discharged into the resistive load. The decay time will be defined based on a best fit to the back side of the pulse measured with the resistive load waveform monitor (paragraph 4.7). This measurement will be used to check on the pulser effective capacitance since the e-fold decay time should be RC where R is the resistive load impedance.

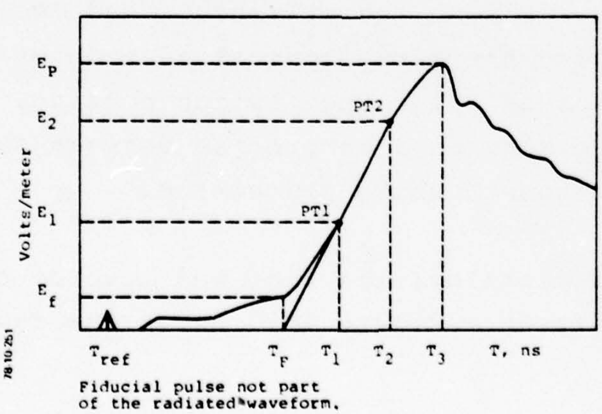

Figure 4 (This waveform is reproduced from the Air Force statement of work quoted here.)

4.2 ACCEPTANCE TESTS

Acceptance testing started as planned and the pulse generator was operated at the one-third and two-thirds peak voltage levels, 20 discharges at each level, without malfunction. After raising the peak voltage to the 4.0-MV level, the monitored signal from the peaking capacitor probe indicated that dielectric breakdowns were occurring. Figure 4-9 illustrates a normal discharge voltage and a breakdown condition at approximately 400 ns after peak voltage.

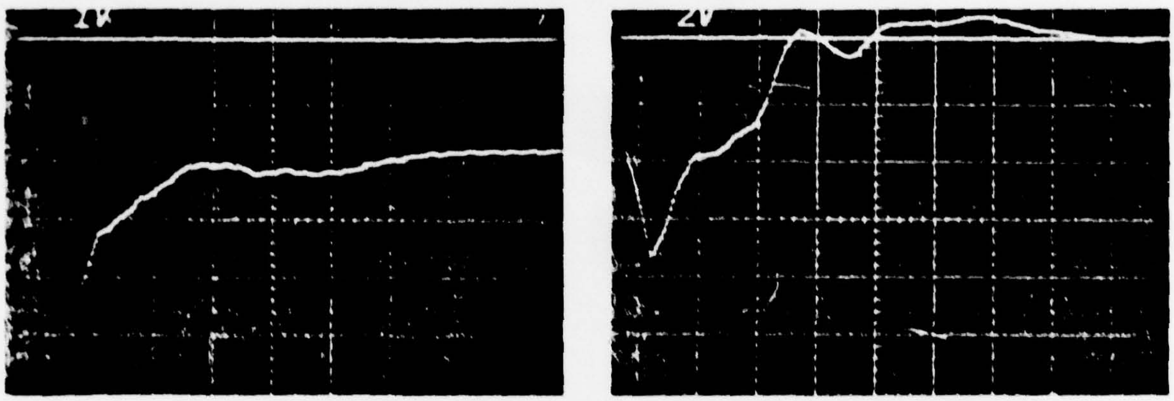

Normal   Breakdown

Figure 4-9 E-field probe waveforms, 4.0 MV.

On inspection it was seen that flashover had occurred between the protective ring and the first conical section of the antenna, across the surface of the output switch housing. A decision was made to lower the ring as a compromise between system voltage capability and switch housing protection.

After field plotting, the ring was lowered by 6 inches from its original position. Figure 4-10 shows the revised field conditions.

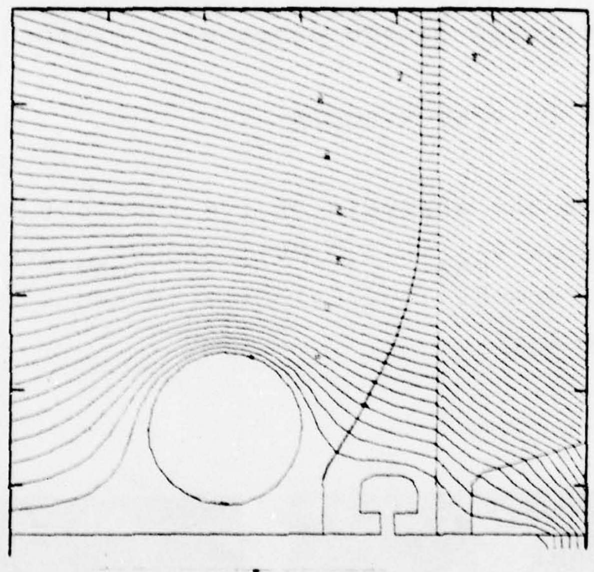

78-10-248

Figure 4-10 Equipotential plot showing VPD 8-inch ring lowered 6 inches.

The acceptance tests were resumed on 27 April 1978, with the revised protective ring in position. Again, late-time breakdowns occurred in the peak voltage range from 4.0 to 4.2 MV. At this point an Air Force decision was made to restrict the upper voltage level of testing to 4.0 MV and the maximum voltage acceptance criterion was revised from 5.0 MV to 4.0 MV. Under these conditions, the testing program was completed on 5 May 1978.

Subsequent inspection of the pulser showed that breakdown streamers had moved across the epoxy/gas interface of the peaking capacitor. These streamers caused sites of charge concentration on the inner wall of the switch housing and some consequent tracking. All these superficial damage areas were cleaned and repaired.

4.4 TABULATION OF TEST RESULTS

Tabulations and analysis of the test data for 1/3 V_{max}, 2/3 V_{max} (based on V_{max} = 5.0 MV), and V_{max} are presented in Tables 5, 6, 7, and 8. Typical E-field and B waveforms are given in Figure 4-11.

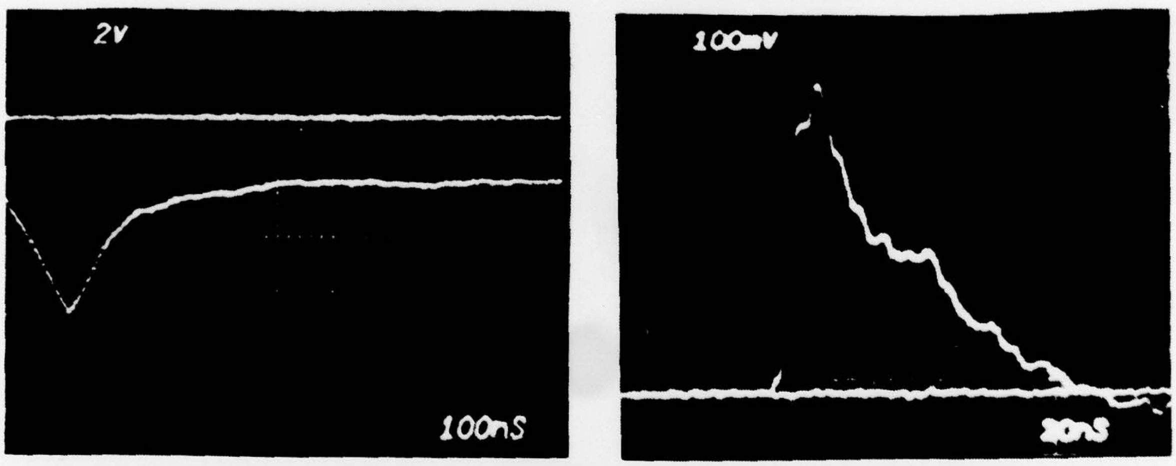

E-field monitor $\dot{B}$ probe

Figure 4-11 Typical E-field and $\dot{B}$-probe waveforms.

4.5 AIR FORCE COMMENTS ON VPD-II ACCEPTANCE TEST RESULTS

Since Air Force personnel assisted in the tests and performed extensive analysis of the test data, their description of the tests and comments upon the results are included here:

> The acceptance test was organized in two parts: the operational test and the high-frequency test. Operational testing consisted of short circuit, open circuit, and aximuthal symmetry tests and a series of 20 firings at 1.7 MV, 3.4 MV, and 4.0 MV. At each level, peak amplitude, self-fire and pulse repetition rate were observed. The high-frequency test was to determine the early time characteristics of the pulser system, risetime and its associated jitter, peak amplitude and its variation, inflections on its rise-front prepulse and time delay jitter.
>
> Testing began 18 April 78 at 1/3 V_{max}, 1.7 MV. Originally 5 MV was the maximum output level; however, during preliminary testing, maximum output was reduced to 4 MV. The one-third and two-thirds test voltage levels remained at 1.7 and 3.4 MV. Prior to acceptance test the pulser system was operated at 5 MV. This voltage level placed a severe field stress on the lower flange of the output switch housing, resulting in a repairable failure. To relieve the field stress a grading ring was placed around the lower flange. This modification had the effect of limiting the output voltage to a nominal 4.3 MV. Operation is erratic at this level. An arc occurs soon after switch closure between the grading ring and conic transition section above the output switch thus limiting the maximum output level. Stable operation (jitter within spec) was achieved at a nominal 4.0 MV.
>
> The following sensors were used:
>
> At the peaking capacitor: The pulser system has a built-in $\bar{E}$-field sensor in the peaking capacitor outer conductor. The calibration factor is 4.07 volts per megavolt. A 1-ns integrator was used.
>
> At 50 meters: The VPD-II has two permanent sensors located at the edge of the test pad, a distance of 50 meters from the output switch center. The sensors are a MGL-4G(R) (B-dot) and a HSD-IB(A) (D-dot). Ten μs integrators used with 50 meter data. A "Power Tee" was used on some of the peaker

data and some of the B-dot data. It appears that whenever the divider was in the line, the waveforms shown on the oscillographs were slightly smaller than they should be. This is to say that the signal divider is supposed to be attenuating the signal by 50 percent but is actually attenuating it by more than 50 percent, which can be seen in comparison of the 20 shots taken at full voltage (with the divider in the line) with the 50 shots taken at full voltage (without the divider). An error of as much as 2.5 percent is observed.

At 10 meters: The azimuthal test was conducted at a radius of 10 meters with two MGL-5(R).

To summarize the operational test, there were no self-firings (spec stipulates one in twenty) at either 1.7, 3.4 or 4.0 MV. Twenty firings were completed at each voltage level. The pulse repetition rate was within specification. The peak voltages at each level was measured by the peaking capacitor monitor and determined by the $\bar{E}$-field measurement (at 50 meters) times the distance to the switch.

Voltage Level, MV	Peaker, MV	$\bar{E}$r Product, MV
1.7	1.703	1.686
3.4	3.220	3.425
4.0	3.999	4.147

The short circuit, open circuit and azimuthal symmetry tests were successfully completed. To accomplish the short circuit test, the output was shorted at the transition section/antenna interface. The open-circuit condition was achieved by firing the pulser system at 1.7 MV with a switch gap spacing that would not break down. The open circuit decay was greater than the required 10 ns. The azimuthal symmetry test used two sensors, one fixed and the other rotated around the output switch. Both were at a radius of 10 meters. After each firing the data was compared and was within the 5 percent requirement.

The high-frequency test was a series of 50 successful firings at 4 MV. The pulser system risetime, peak voltage, time delay jitter and prepulse were determined by taking the fastest 50 percent of the rise and doubling it. The risetime fell between 7.4 ns and 8.6 ns, for a mean of 8.0 ns. This met the 10 ns t_r and Δt_r specification. A risetime of 10 to 90 percent is also included in the attached data. Peak output amplitude was determined by $\bar{E}$r product 4.17 MV and as measured at the peaker, 4.14 MV. The rms of the series was also 4.14 MV. The peak amplitude and amplitude variation requirements are met. Time delay jitter was determined by determining the standard deviation of the time to peak voltage for the

series. The requirement was that the standard deviation be less than 10 ns. It was determined to be 6.9 ns. The prepulse was measured at 50 meters and typically 7.5 percent, well below the 20 percent maximum. The rise front is smooth to the 90 percent point where an inflection occurs. It is not readily apparent what is causing this inflection. At this point it does not appear to documentally affect performance of the pulser system.

In conclusion the VPD-II pulser system performed satisfactory and met the intent of the SOW with the exception of 5 MV level of operation.

TABLE 3

EQUATIONS/DEFINITIONS

(1) Risetime (t_r)

$$t_r = 2\,(t_2 - t_1) \leq 10 \text{ ns}$$

where

$$|E_2 - E_1| \geq |1/2(E_p - E_o)|$$

$$\Delta t_{r(max)} \leq 2 \text{ ns}$$

(2) Jitter (t_j)

$$t_j = \sqrt{1/n \sum_{i=1}^{n} (t_p - t_m)^2}$$

where t_m is the aritmetric mean of $(t_p - t_{ref})$ for n shots.

(3) Antenna resistive loading per unit length

$$R(z) = Z_\infty \left[\frac{1}{h-z}\right]$$

where Z_∞ = 120 ohms

(4) Prepulse < 20% of E_p

$$|E(t)|_{max} \leq 0.2\, E_p \text{ for } 0 < t \leq t_f$$

(5) Time of output switch firing, t_f This term is defined as the intersection of two lines, the base line and a line defined by points (E_2, t_2) and (E_1, t_1) on the risefront of the time domain waveform.

TABLE 4

ACCEPTANCE TEST DATA
OPERATIONAL TEST 1/3 V_{max}

Shot Number	Peak $\dot{B}$ cm	Peak $\dot{B}$ kV/m	t_j(ns)	t_r 10-90%(ns)	t_r Fast 50%(ns)	Peaker Amplitude (MV)
21	5.65	33.90	31.5	6.0	6.4	1.708
22	5.55	33.30	32.9	6.2	6.3	1.700
23	5.65	33.90	31.0	5.9	6.2	1.705
24	5.57	33.42	31.8	5.9	6.2	1.698
25	5.64	33.84	34.4	5.9	6.0	No Picture
26	5.60	33.60	22.0	6.0	5.8	1.705
27	5.62	33.72	31.6	5.9	6.2	1.695
28	5.63	33.78	30.3	6.3	6.4	1.705
29	5.65	33.90	23.3	5.7	6.0	1.700
30	5.61	33.66	32.7	6.0	6.4	1.715
31	5.64	33.84	32.4	5.8	6.2	1.715
32	5.58	33.48	32.4	6.2	6.4	1.715
33	5.58	33.48	24.8	5.5	6.6	1.690
34	5.67	34.02	28.4	5.6	6.0	1.710
35	5.68	34.08	30.4	5.8	6.4	1.710
36	5.62	33.72	24.5	5.8	6.4	1.710
37	5.59	33.54	31.6	6.2	6.6	1.715
38	5.56	33.36	28.2	5.7	6.0	1.695
39	5.55	33.30	22.0	6.0	6.4	1.690
40	5.77	34.62	15.9	5.0	5.8	1.670
MEAN	5.62	33.72	28.6	5.9	6.2	1.703

$\Sigma\ t_j = 448.15 \qquad \sigma = 4.86 = t_j$

$\bar{E}_r$ = (33.72 kV/m) (50 m) = 1.686 MV

T_j - jitter

TABLE 5

ACCEPTANCE TEST DATA
OPERATIONAL TEST 2/3 V_{max}

Shot Number	Peak $\dot{B}$ cm	Peak $\dot{B}$ kV/m	t_r: t_j(ns)	t_r: 10-90%(ns)	t_r: Fast 50%(ns)	Peaker Amplitude (MV)
78	4.8	72.0	33.2	10.0	8.0	3.27
79	4.6	69.0	41.8	9.8	8.0	3.19
80	4.7	70.5	45.2	9.8	7.8	3.24
81	4.65	69.8	36.6	9.8	8.0	3.22
82	4.4	66.0	39.2	10.2	9.8	3.17
83	4.5	67.5	37.0	10.4	7.8	3.24
84	4.7	70.5	38.0	10.2	8.2	3.29
85	4.45	66.8	27.7	9.8	8.0	3.10
86	5.7	70.5	37.2	9.8	8.0	3.32
87	4.6	69.0	32.5	10.0	8.0	3.22
88	4.4	66.0	29.0	10.2	9.8	3.10
89	4.45	66.8	36.7	10.5	10.0	3.10
91	4.5	67.5	32.4	10.5	8.8	3.22
92	4.7	70.5	41.4	9.8	8.2	3.32
93	4.3	64.5	17.3	10.3	7.8	3.15
94	4.6	69.0	39.0	10.2	7.8	3.24
95	4.6	69.0	34.2	10.0	8.0	3.27
96	4.7	70.5	22.6	10.4	7.8	3.22
97	4.7	70.5	33.0	10.3	8.0	3.32
MEAN	4.6	68.5	33.8	10.2	8.4	3.22

$\Sigma\ t_j = 972.77 \quad \sigma = 7.15 = t_j$

$E_r = (68.5\ \text{kV/m}) \quad (50\ \text{m}) = 3.425\ \text{MV}$

TABLE 6

ACCEPTANCE TEST DATA
OPERATIONAL TEST FULL VOLTAGE

Shot Number	Peak $\dot{B}$ cm	Peak $\dot{B}$ kV/m	t_j(ns)	t_r 10-90%(ns)	t_r Fast 50%(ns)	Peaker Amplitude (MV)
190	5.67	85.0	39.3	9.7	8.0	4.128
191	5.57	83.6	48.5	10.0	8.0	4.079
192	5.6	84.0	46.0	10.0	7.6	4.029
193	5.67	85.0	51.0	9.5	7.6	4.177
194	5.5	82.5	29.2	9.9	8.0	4.000
195	5.56	83.5	33.3	10.0	8.0	4.029
196	5.47	82.1	36.5	10.2	7.6	3.97
197	5.43	81.5	26.5	10.2	5.4	3.892
198	5.5	82.5	35.5	10.0	7.6	4.020
199	5.5	82.5	42.4	10.2	7.6	4.020
200	5.46	82.0	34.0	9.7	7.8	4.010
201	5.63	84.5	37.3	9.7	7.8	4.029
202	5.4	81.0	22.0	10.0	8.0	3.813
203	5.43	81.5	37.5	10.3	7.6	3.822
204	5.45	81.75	42.4	10.0	8.4	4.029
205	5.53	82.95	37.6	11.3	7.8	4.059
206	5.46	81.9	27.8	10.0	7.8	3.931
207	5.54	83.0	33.4	10.0	7.6	4.000
208	5.5	82.5	41.8	10.0	8.0	4.010
209	5.45	81.75	31.0	10.0	8.0	3.941
MEAN	5.53	82.94	36.6	10.0	7.8	3.999

$\Sigma\, t_j = 733 \quad \sigma = 7.43 \text{ ns} = t_j$

$\bar{E}_r = (82.94 \text{ kV/m}) \quad (50 \text{ m}) = 4.147 \text{ MV}$

TABLE 7

ACCEPTANCE TEST DATA
HIGH FREQUENCY TEST
50 SHOT SERIES AT 4 MV

Shot Number	Peak B cm	Peak B kV/m	t_j (ns)	t_r 10-90% (ns)	t_r Fast 50% (ns)	Peaker Peak Amplitude (MV)	Peak D Field (kV/m)
211	5.5	82.5	36.5	10.3	7.6	4.07	73.5
212	5.57	83.6	54.5	10.0	8.0	4.13	73.8
213	5.57	83.6	41.4	10.2	7.8	4.20	74.7
214	5.54	83.1	51.3	9.7	8.0	4.18	74.5
215	5.48	82.2	48.7	10.4	8.4	4.16	74.2
216	5.48	82.2	48.7	10.4	8.0	4.00	72.8
217	5.56	83.4	42.4	9.8	8.4	4.07	73.5
218	5.57	83.6	51.8	10.0	7.8	4.19	
219	5.61	84.2	51.0	10.0	7.8	4.19	75.0
220	5.58	83.7	36.7	10.5	7.8	4.04	73.8
221	5.42	81.3	36.0	10.4	8.0		72.5
222	5.5	82.5	41.2	10.4	8.4	4.08	72.9
223	5.7	85.5	47.6	9.7	7.6	4.23	76.8
224	5.66	84.9	51.6	10.0	8.0	4.17	74.4
225	5.5	82.5	31.7	10.4	8.0	4.04	72.1
226	5.6	84.0	34.4	10.5	8.2	4.09	73.8
227	5.6	84.0	41.8	10.0	8.2	4.12	73.7
228	5.57	83.6	52.3	9.8	7.6	4.10	74.1
229	5.65	84.8	51.7	9.4	7.4	4.21	75.9
230	5.6	84.0	48.9	10.0	8.0	4.30	74.9
231	5.64	84.6	42.5	10.1	7.6	4.17	74.6
232	5.57	83.6	47.1	10.4	7.8	4.15	74.7
233	5.3	79.5	39.2	10.1	7.4	3.89	70.5
234	5.58	83.7	52.5	10.1	8.6	4.19	74.4
235	5.62	84.3	52.7	10.2	8.0	4.17	74.8
236	5.63	84.5	40.7	10.3	8.0	4.18	74.6
237	5.64	84.6	48.4	10.2	7.4	4.17	74.8
238	5.58	83.7	44.9	10.2	8.0	4.21	74.7
239	5.63	84.5	47.7	10.3	7.8	4.18	74.8
240	5.6	84.5	48.0	10.5	8.0	4.21	74.6

TABLE 7 (cont.)

Shot Number	Peak $\dot{B}$ cm	Peak $\dot{B}$ kV/m	t_j(ns)	t_r 10-90% (ns)	t_r Fast 50% (ns)	Peaker Peak Amplitude (MV)	Peak D Field (kV/m)
241	5.56	83.4	31.7	10.6	8.2	3.96	72.2
242	5.74	86.1	54.0	9.9	8.0	4.22	76.5
243	5.54	83.1	41.0	10.4	7.6	4.10	73.8
244	5.45	81.8	34.8	10.7	8.4	3.98	71.5
245	5.56	83.4	50.5	10.2	8.2	4.17	73.7
246	5.56	83.4	38.4	10.3	8.4	4.14	73.5
247	5.45	81.8	44.7	10.5	8.2	4.03	72.6
248	5.6	84.0	48.5	10.1	8.2	4.18	74.4
249	5.64	84.6	53.1	9.7	7.6	4.26	75.6
250	5.53	83.0	43.0	10.4	8.4	4.13	73.6
251	5.48	82.2	50.6	10.5	8.4	4.12	72.9
252	5.61	84.2	55.1	10.1	7.8	4.18	74.5
253	5.47	82.1	56.0	10.4	8.0	4.25	73.7
254	5.55	83.3	49.2	10.0	8.0	4.18	74.2
255	5.58	83.7	61.8	9.7	7.4	4.22	75.2
256	5.63	84.5	47.2	10.2	7.6	4.13	74.2
257	5.57	83.6	46.1	10.4	8.0	4.18	74.9
258	5.5	82.5	49.2	10.3	8.0	4.13	73.8
259	5.5	82.5	57.0	10.7	8.2	4.16	73.7
260	5.54	83.1	44.4	10.2	8.6	4.07	73.5
MEAN	5.57	83.5	46.4	10.2	8.0	4.14	72.7

$\Sigma\, t_j = 2331 \quad \sigma = 6.9 \text{ ns} = t_j$

$\bar{E}_r = (83.5 \text{ kV/m}) \quad (50 \text{ m}) = 4.175 \text{ MV}$

SECTION 5

SUMMARY AND CONCLUSIONS

The VPD II pulse generator has performed and will perform in a satisfactory manner within the peak voltage restoration of 4.0 MV.

Since the Marx generator has been designed for a maximum operating output voltage of ~ 6 MV, there are possibilities for up-grading the overall system voltage performance if there is a need.

The present limitations are confined to the dielectric capabilities of the output switch housing and the upper slab of the peaking capacitor which is mounted to the lower electrode of the output switch. The outer surface of the former operates with stmospheric (5000 ft) Freon R12 and the latter with 40 psig SF_6.

The evidence suggests that both these surfaces are limited at ~ 4.0 MV, although there is a possibility that a surface discharge on one could initiate a discharge on the other.

Broadly, there are two possible approaches to upgrading:

i) To consider a basic redesign of the output peaking circuit, from the peaking capacitor assembly to the conical section.

ii) To retain the present design configuration of the peaking circuit and improve the critical dielectric surfaces by design refinements and relatively modest modifications.

The former approach could ensure full exploitation of the Marx generator but at considerable cost.

The outcome of the second approach is less certain but there is a reasonable expectation that a reliable 4.5 MV operational level could be achieved at least. The cost for this route would be much lower and the work could proceed in convenient phases.

It is apparent in this report that the output switch housing and the peaking capacit or upper epoxy slab have been prone to surface and, in the case of the housing, volume failure between 4.0 to 5.0 MV, even under dummy loading conditions. Design and constructional improvements have not been adequate to raise system performance under the conditions of the extended pulse decay periods which are characteristic of the antenna load.

For these conditions when the decay of the output voltage extends to microseconds it seems more reasonable to base the design electrical stresses upon the following exponential waveform rather then the rising waveform.* If this is done for the switch housing it can be confirmed that the surface can flash over in one atmosphere of Freon R-12, 5000 ft at 4.0 MV. It requires 760-mm ambient pressure of R-12 to support the decay from 5.0-MV peak. An inflatable dielectric housing, surrounding the output switch fiber-glass housing, could provide this required pressure differential of R-12 for the fiber-glass and have adequate flash-over path length itself for the lower ambient pressure.

*Crewson, U., Point-Plane Spark Gaps - A Technical Report, Pulsar Assoc., PAR 71-5.

The geometry of the peaking capacitor slab could be evaluated for improved surface flash-over performance. This, coupled with refinements to the switch housing stress-relieving ring, which influences the dielectric performance of both the housing and peaking capacitor slab.

In summary, extended operation of the VPD II will establish that maximum peak voltage operation at the 4.0 MV level is realistic. If an upgrading of his performance is required in the future, there are a number of actions which can be taken to meet the requirements.